The Impact of LFH Mineral Mix on the Function of Reclaimed Landscapes in the Athabasca Oil Sands Region, Alberta, Canada

by

Hilary Irving

A thesis
presented to the University of Waterloo
in fulfillment of the
thesis requirement for the degree of
Master of Science
in
Geography (Water)

Waterloo, Ontario, Canada, 2020

AUTHOR'S DECLARATION

I hereby declare that I am the sole author of this thesis. This is a true copy of the thesis, including any required final revisions, as accepted by my examiners.

I understand that my thesis may be made electronically available to the public.

Abstract

The Athabasca Oil Sands Region (AOSR), located within the Western Boreal Plains (WBP) is characterized by a mosaic of boreal uplands and peatlands that dominate the terrain. These landscapes are underlain by oil-bearing formations (bituminous sands) and are disturbed or completely removed during resource exploration and extraction. Oil companies operating in the AOSR are mandated by the Government of Alberta to return their leased lands to an equivalent land capability. In doing so, new landscapes are constructed using materials salvaged from the pre-mined landscape and by-products from the mining process itself. Successful reclamation rests on an understanding of the soil physical properties that characterize these materials and how they impact intended function, both at the time of placement and in later years of reclamation. This research specifically focuses on the use of LFH mineral mix (hereafter referred to as LFH) as a cover soil in reclaimed landscapes and how its properties impact functionality.

The temporal evolution of LFH was assessed using six reclamation study sites of six distinct ages (4 years post reclamation – 11 years post reclamation). A series of soil physical properties were analyzed in the top 10 cm of the LFH profile and while certain properties did follow a trend with time, other properties were likely an intrinsic property of the LFH upon placement. The dynamic nature of LFH captured within the time frame of this study contributes to an improvement in hydrological response with time (increasing α and maximum infiltration rates). Properties such as soil organic matter and bulk density, that would less readily change under biotic and abiotic forces impact the initial quality of LFH upon placement. And, while higher initial quality does improve the likelihood of success in early years of reclamation, sites of lower initial quality still performed as intended. Considering the entire soil profile, LFH over subsoil (glacial till or tailings sand) is likely to form a percolation barrier. The presence of these barriers (hydraulic or capillary) can be detected using easily obtained soil physical properties and they should be considered along with the intended function of a reclaimed landscape. Both types of barriers can benefit vegetation as water is held above the interface of the two materials, increasing field capacity and thus available water holding capacity. However, their behaviour in relation to increasing soil moisture conditions differs. While a hydraulic barrier is weakened, allowing more water to steadily move beyond the interface, a capillary barrier is broken through, and the two materials remain hydraulically connected until the barrier is restored. The behaviour of a capillary barrier could benefit landscapes where percolation into the subsurface is crucial to success.

Acknowledgements

Many people from the last three years deserve recognition as I could not have gotten here without them – but there are a few in particular I would like to point out.

First – thank you to my supervisor Dr. Jonathan Price for providing such a valuable opportunity and wonderful space to learn. I have gained so, so much along the way. Thank you!

Next, I would like to thank my fellow students and colleagues in the Wetlands Hydrology and Hydrometeorology Labs at Waterloo. Thanks to James Sherwood, Eric Kessel and Owen Sutton for all the advice, assistance and support in the field and lab – and understanding what all those results meant. Nataša Popović - your presence in Fort McMurray kept me sane and fed. And to all those that lent a helping hand with field work – especially Tyler Prentice and Gabriel Dubé.

Thank you to my wonderful friends and family. Mom, you have stood behind all my decisions with unwavering support – I am proud to be your daughter.

And finally, my husband Tom. You are one of a kind and it would be impossible to put into words how much your endless love and support mean to me. I can't wait for whatever is next.

Dedication

To my Dad, Stephen. I have carried with me the spirit and positivity you left in this world and will continue to do so wherever I go. I am lucky to have known you. Cheers to you.

Table of Contents

List of Figures

List of Tables

Chapter 1
Introduction

1.1 Land reclamation in the AOSR

The Athabasca Oil Sands Region (AOSR), located within the Western Boreal Plains (WBP) is characterized by a mosaic of boreal uplands and peatlands that dominate the terrain (Zoltai et al., 1988). These landscapes are underlain by oil-bearing formations (bituminous sands) and are disturbed or completely removed during resource exploration and extraction (Government of Alberta, 2019). As of 2016, open pit mining activities, which are employed to extract shallower (< 75 m bgs) oil sands, have resulted in the complete removal of 901 km^2 of the landscape and associated ecosystem services (Alberta Environment, 2019). Oil companies operating in the AOSR are mandated by the Government of Alberta to return their leased lands to an equivalent land capability (Alberta Environment, 2010). This involves reconstructing entire landscapes that support land uses with similar functions to those that existed prior to disturbance, but that are not necessarily identical (Alberta Environment, 2010). Several decades of research dedicated to the development of techniques to re-build landscapes that meet these regulatory requirements have resulted in a post-disturbance landscape that incorporates materials from the pre-disturbed landscape and by-products from the mining process itself. After placement, these materials (*e.g.* cover soils) develop over time as a result of biotic and abiotic forces that alter their physical, chemical and biological properties (Karlen et al., 2003). This can have an important influence on the functionality of a reclaimed system over time, yet the rates and character of these changes have not been sufficiently established for the range of materials used for reclamation.

The process of open pit mining results in large piles of overburden, the material originally between the uppermost organic and mineral horizons and the underlying oil-bearing sands that are collected for processing, and tailings sand resulting from that processing. Both overburden and tailings sand are used in the construction of new landscapes. Overburden is formed into upland formations know as overburden dumps, and tailings sand is used to construct dikes, which surround tailings ponds. These landscapes are capped with an arrangement of cover soils intended to support the establishment and growth of upland boreal vegetation, and aid in the containment of naturally occurring solutes, such as sodium, associated with the overburden and tailings sand (Elshorbagy et al. 2005; Huang et al., 2013; Kelln et al, 2007). Two materials commonly used as a cover soil in the AOSR are peat-mineral mix (hereafter called PMM) and LFH-mineral mix (hereafter called LFH).

PMM is salvaged from low-lying areas where fens and bogs are found and includes the organic peat layer and varying proportions of the underlying mineral horizons (Mackenzie, 2011). Once trees have been cleared, LFH is salvaged from upland areas and contains the intact, partially decomposed and decomposed organic layers (litter, fibric and humic, respectively) and variable proportions of the underlying A and B mineral horizons (Naeth et al., 2013). Materials placed between toxic (saline-sodic) overburden and the final capping layer include glacial and lacustrine till (Mackenzie, 2011). These materials, referred to as subsoils, protect the rooting zone from upward diffusion of contaminants from below (Kessler et al., 2010) while also acting as a barrier to mitigate downward percolation (Meiers et al., 2011b).

Upland cover soils play a key role in the functionality of a reclaimed landscape; success in reclamation rests on an understanding of how their properties influence intended outcomes. PMM and LFH vary considerably in their physical, chemical and biological properties, however some general assumptions can be made when comparing the two. For instance, PMM typically has greater soil organic matter (SOM), which confers higher soil water retention (Naeth et al., 2013). In a study that estimated percolation as a percentage of precipitation, Barber et al. (2015) found that on average, experimental plots capped with PMM had net percolation rates of 14% compared to those capped with LFH at 23%. Nevertheless, LFH has been consistently shown to be a more effective substrate for revegetation, despite its weaker soil-water retention. Sites capped with LFH have a more diverse vegetation community compared to PMM (Dhar et al., 2018), as well as lower seedling mortality rates (Barber et al., 2015). Salvaged LFH consists of a propagule bank that assists in natural recovery (Mackenzie & Naeth, 2010) and has more favourable soil nutrient regimes (Jamro et al., 2014). In addition, the interaction between a cover soil and its underlying subsoil influences the way a reclaimed landscape functions. Capillary barriers, which are created when a finer soil is layered over a coarser soil, have been noted in landscapes capped with both LFH and PMM (Leatherdale et al., 2012; Naeth et al., 2011; Sutton & Price, 2019). In the presence of a capillary barrier, field capacity in the cover soil may be higher than in a homogenous profile (Huang et al., 2013). This contributes to a higher available water holding capacity (AWHC), which represents the amount of water available to plants and is the difference between field capacity and permanent wilting point.

Though PMM and LFH are both suitable upland cover soils, a greater understanding of their variability, and the impact this has on intended functionality, is needed. Some of this variability lies in quality upon salvage or placement. A soil's quality is largely dependent on its ability to perform in the way it was intended (*e.g.* support upland vegetation and restrict percolation) (Karlen et al., 2003).

Although suitable levels of quality have been defined for materials used in reclamation (Alberta Environment, 2006), they do not consider how a soil may change post-placement. Studies that have tracked the hydrophysical evolution of PMM have noted changes to properties such as an increase in infiltration capacity, which alters its hydrological response (Kelln et al., 2007; Meiers et al., 2011). In reclamation landscapes built with the intention of restricting percolation, this could potentially pose a problem as the landscape ages. Conversely, more novel landscapes could benefit from the same result. For example, in 2012 an upland-fen watershed, known as the Nikanotee Fen Watershed (NFW), was constructed to test the feasibility of fen reclamation in the post-mined landscape. Since fens rely on groundwater inputs from their adjacent uplands, the upland portion of the landscape must support the establishment and growth of vegetation while also promoting groundwater recharge (Ketcheson et al., 2017).

1.2 Objectives

The use of appropriate soil prescriptions is essential in achieving the intended functionality of a reclaimed landscape. The performance of soil prescriptions used in typical reclamation landscapes (*e.g.* overburden dumps) have been well documented (*e.g.* Huang at al., 2015; Meiers et al., 2011; Naeth et al., 2011); however, these often intentionally limit the movement of water below their cover soils. With recent research efforts focused on the construction of upland-fen watersheds it is necessary to understand how upland cover soils (*e.g.* LFH mineral mix) may impact the functionality of a landscape where hydrological connectivity between its units (upland surface, aquifer, fen) is crucial to its success. Although LFH has been shown to be an effective substrate for re-vegetation (*e.g.* Naeth et al., 2013), a greater understanding of its hydrophysical properties and how they may impact reclamation landscapes is necessary. Therefore, the primary objectives of this thesis are to:

1) Track the evolution of LFH in the context of its hydrophysical properties;
2) Evaluate the movement of water through LFH into its underlying subsoil, focusing on the interface between the two materials and discuss the implications on groundwater recharge;
3) Assess whether LFH has the capacity to function successfully as the upland cover soil in an upland-fen watershed.

1.3 Thesis format and project role

This thesis includes two manuscript style chapters entitled Chapter 2: The hydrophysical evolution of LFH-mineral mix in the post-mined landscape; and Chapter 3: Implications of LFH-mineral mix in a layered soil profile. Chapter 2 used six study sites that differed in age to characterize the changes LFH undergoes post-placement and includes a mix of both field and laboratory data. Chapter 3 used laboratory column experiments to assess the movement of water through LFH and into its underlying material (tailings sand, overburden). My role for this project included research design in collaboration with my supervisor, field data collection, laboratory analysis, data analysis and writing the first draft of all chapters, after which feedback and revisions from my supervisor and committee were incorporated prior to submitting a finalized copy.

Chapter 2
The hydrophysical evolution of LFH-mineral mix in the post-mined landscape

2.1 Introduction

In the Athabasca Oil Sands Region (AOSR) lands disturbed by mining activities must be returned to an equivalent land capability through land reclamation activities (Alberta Environment, 2010). Reclamation landscapes employ a variety of materials from the pre-disturbed landscape and by-products of the mining process itself. Use and placement of the appropriate materials is essential to successful reclamation, and these differ depending on the intended functionality of the reclaimed landscape. For instance, typical upland reclamation landscapes where sustainable re-vegetation is the primary goal, are designed to limit percolation to mitigate the movement of contaminants contained within the underlying overburden (Kelln et al., 2007). This is achieved by layering soils in a manner that ensures soil water is held near the surface and thus available for vegetation (Huang et al., 2013). More recent efforts in reclamation include the construction of an upland-fen watershed, known as the Nikanotee Fen Watershed (NFW). Since fens rely on groundwater inputs from their adjacent uplands, the NFW's upland cover soil must be able to support vegetation growth while also promoting recharge into its underlying aquifer (Ketcheson et al., 2017). Choosing an appropriate cover soil to support vegetation, prevent percolation or promote recharge rests on an understanding of how soil properties impact the intended functionality of a reclaimed landscape.

Soil can be broken down into physical, biological and chemical properties that are either inherent to the soil or dynamic in nature. Inherent properties (*e.g.* soil texture) remain relatively stagnant with time, while dynamic properties (*e.g.* infiltration capacity) change under the influence of biotic and abiotic forces (Karlen et al., 2003). Successfully achieving the intended functionality of an upland in a constructed upland-fen watershed will in part depend on the temporal trajectory of the cover soil's hydrophysical properties. In reclamation, salvaged soils that are placed to act as a growing substrate, such as LFH mineral mix (hereafter called LFH), can initially be of poor quality due to the salvaging process that alters its physical properties (structure, bulk density, available nutrients, *etc*.). Poor physical quality in early years of reclamation can result in low infiltration and high runoff rates (Ketcheson, 2015); however, with time, quality has been shown to improve. Benson et al. (2007) found that the hydraulic conductivity of cover soils used in waste containment systems

with initially very low values (10^{-9} m s^{-1}) increased between one and four orders of magnitude within two years. Guebert & Gardner (2001) found that within four years of reclamation, infiltration rates of reclaimed mine soils in Pennsylvania increased from 5.5 x 10^{-6} m s^{-1} to pre-disturbance rates of 2.2 x 10^{-5} m s^{-1}. In the AOSR the hydraulic conductivity of a peat-mineral mix (PMM) substrate increased by one order of magnitude (8 x 10^{-6} m s^{-1} to 7 x 10^{-5} m s^{-1}) within two years of reclamation, and plateaued or decreased slightly thereafter (Meiers et al., 2011). Using numerical modelling, Sutton & Price (2019) suggest that weathered LFH (due to freeze-thaw cycling) had a hydraulic conductivity one order of magnitude higher than in its un-weathered state.

In contrast to the studies mentioned above that tracked the development of one soil over the course of several years, others have used space for time, or a chronosequence, to study the evolution of reclaimed landscapes over time. Sorenson et al. (2011) studied the influence of stand type on forest floor development and soil microbial communities and what, if any, the influence of time since reclamation had on these relationships. Their findings revealed that time was a significant variable for certain stand types, but overall, canopy coverage (independent of time) had the greatest impact on forest floor development and thus the biological functioning of the soil. McAdams et al. (2018) tracked the abundance of a bioindicator in reclaimed soils to determine the influence of time since reclamation on their presence; however, their findings determined that the accumulation of forest floor material was a better predictor than time.

The soil physical properties that control hydrological processes can be expected to follow certain temporal patterns as soils react to abiotic processes, in the form of freeze-thaw and wet-dry cycling (Benson, 1992), and biotic processes, in the form of root proliferation and bioturbation from soil macrofauna (Weiler & Naef, 2003). For example, freeze-thaw cycling has been linked to an increase in hydraulic conductivity in compacted clays (Benson, 1992). Water held within soil expands as it freezes, forcing soil particles to move and thus altering the soil's structure. Upon thaw, voids remain where frozen water was, contributing to an increase in hydraulic conductivity. Similarly, the advancement of roots and filaments of mycorrhizal fungi drives aggregation, and thus an improvement in soil structure (Rillig & Mummey, 2006). These changes may be reflected in the van Genuchten soil water retention curve (Benson et al., 2007; Sutton & Price, 2019), modeled as (van Genuchten, 1980):

$$\boldsymbol{\psi(\theta) = \theta_r + (\theta_s - \theta_r)[1 + (\alpha\psi)^n]^m} \qquad \textbf{Equation 2-1}$$

where ψ is matric pressure (in this form expressed as a positive value representing stronger tension), θ_r is residual water, θ_s is saturated water content, α approximates the inverse of air entry pressure (L^{-}

[1]), *n* is a fitting parameter related to the pore-size distribution and *m* = 1-1/*n*. With time, α should increase, indicating lower air entry pressures due to development of larger pores. Simultaneously, *n* should decrease as the pore-size distribution broadens (Benson et al., 2007; Sutton & Price, 2019).

While the effectiveness of LFH as a substrate for re-vegetation has been very well documented (*e.g.* Mackenzie & Naeth, 2010), studies that track its hydrophysical evolution, similar to those that have tracked PMM (*e.g.* Meiers et al., 2011), are lacking. Understanding the evolution of LFH soils is important to the design of systems relying on groundwater recharge, such as in an upland-fen watershed. Therefore, the objectives of this study are to 1) track the temporal evolution of LFH upland cover soils in the context of their hydrophysical properties and 2) assess whether LFH's physical and hydrophysical properties can support the intended functionality of a cover soil in an upland-fen watershed. The temporal evolution of LFH will be evaluated using space-for-time with a selection of study sites of six distinct ages, capturing the time frame of 4 – 11 years post reclamation.

2.2 Study sites

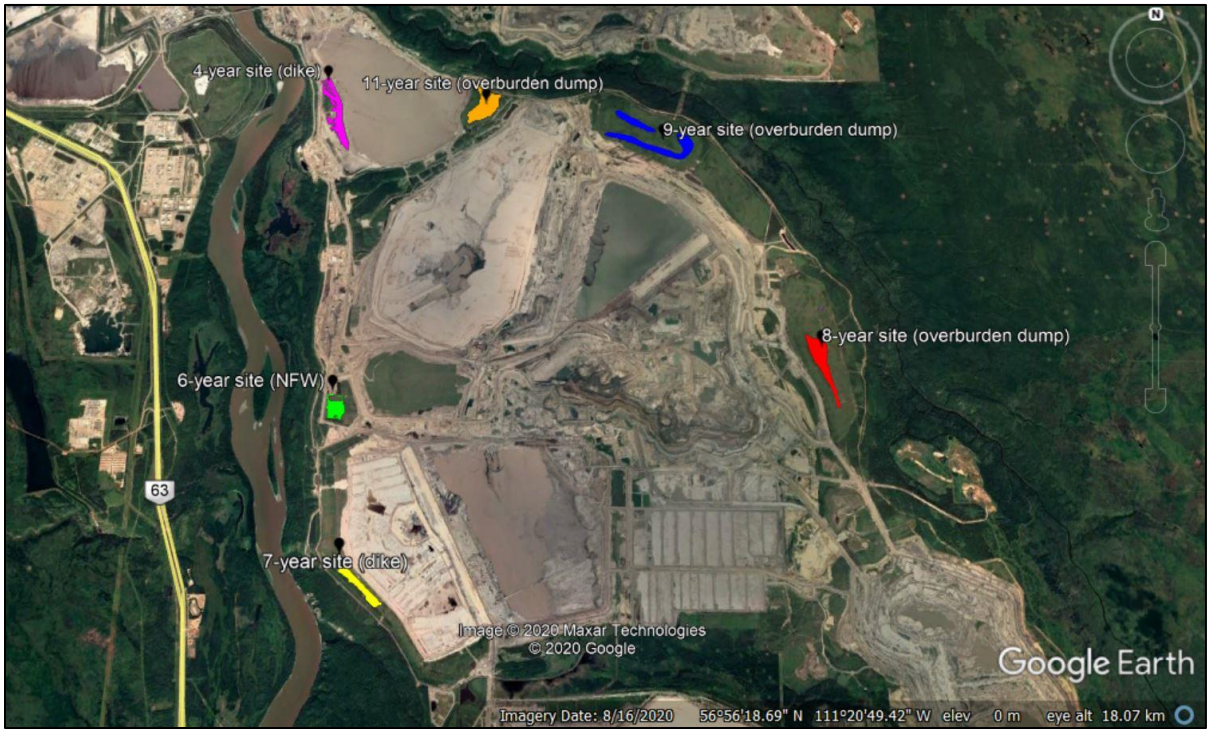

Figure 2-1 – Location of study sites and indication of landform type.

Six reclamation sites located approximately 30 km north of Fort McMurray, Alberta (56°55'52"N, 111°24'59"W) were investigated between May and August of 2018 (Figure 2-1). All sites had been

capped with a layer of LFH the year their respective reclamation began (2014, 2012, 2011, 2010, 2009 and 2007). Thus, for the purposes of this study, these sites were identified as being of six distinct ages (4, 6, 7, 8, 9 and 11-year post reclamation), chosen in an attempt to capture the influence of time on their evolution. The 8, 9 and 11-year sites were overburden dumps constructed using saline-sodic overburden that had been covered with 100 cm of subsoil prior to being capped with LFH. The 4 and 7 – year sites were tailings sand dikes, and the 6-year site was the upland of a constructed fen watershed where the LFH was underlain by a tailings sand aquifer. LFH thickness was approximately 20 cm at the 4, 7, 8, 9, and 11-year sites and approximately 30 cm thick at the 6-year site. LFH placed at the 6-year site originated from a stockpiled source; all other sites received directly-placed LFH.

Following landform construction and LFH placement, each site received several treatments intended to improve the likelihood of success in reclamation. These included fertilizer applications, a nurse crop and surface amendments in addition to planted trees and shrubs. With the exception of fertilizer application, specifics for each treatment varied from site to site. Fertilizer (N-P-K blend of 23.5-35-8) was applied at a rate of 300 kg ha^{-1} the same summer as seedlings were planted. Each site was planted with a mix of native tree species the summer following soil placement, including aspen (*Populus tremulaides)*, balsam poplar (*Populus balsamifera)*, black spruce (*Picea mariana*), white spruce (*Picea glauca*), jack pine (*Pinus banksiana*) as well as an assortment of shrubs, including beaked hazelnut (*Corylus cornuta*), choke cherry (*Prunus virginiana*) and green alder (*Aldus crispa*). The least diverse site at initial planting was the 11-year site, which was planted with only two tree species and five shrub species; the most diverse site was the 8-year site, which was planted with five species of trees and 10 unique shrub species. Initial tree planting densities ranged from 933 – 2797 stems per hectare (SPH) and shrub planting densities ranged from 240-628 SPH. Nurse crops were planted to improve conditions for seedlings by increasing moisture availability during the growing season, and to provide protection from harsh (freezing, snow) conditions during the winter months (Mackenzie, 2011). The 11 and 9-year sites were seeded with a nurse crop of barley, and the remaining (younger) sites were seeded with a mixture of oats and native grasses (*e.g.* slender wheatgrass, Rocky Mountain fescue and tufted hairgrass). Coarse woody debris (CWD) was placed at the 8 and 11-year sites with intended benefits similar to a nurse crop (Brown & Naeth, 2014).

2.3 Methods

To measure soil hydrophysical properties, intact soil samples (10 cm I.D x 10 cm height) were collected from random locations using PVC pipe driven carefully into the ground. Recovered samples (n = 9, all sites) were then wrapped tightly with plastic film and were refrigerated until laboratory analysis could take place. An additional five samples (10 cm I.D x 20 cm height) were collected from five randomly selected locations at each site to determine fine root biomass. In-situ infiltration rates were measured at the surface using randomly placed single-ring infiltrometers (# of samples ≈ 35, all sites). Tree height and density surveys were also completed using five randomly placed 10 m x 10 m plots at each site. All trees located within each plot were assessed for height, diameter at breast height (DBH) and species type.

The intact soil samples were sub-sampled in the laboratory using stainless steel rings to produce smaller intact cores (8 cm I.D x 5 cm height), with the leftover sample stored separately. The smaller intact cores were used to measure saturated hydraulic conductivity (K_{sat}), soil-water retention, bulk density and porosity. K_{sat} was measured using the KSAT System (Meter Group) using the falling head method, derived from Darcy's law,

$$\boldsymbol{q = \frac{Q}{A} = -K_{sat}\frac{dh}{dl}} \qquad \textbf{Equation 2-2}$$

where q is the specific discharge (L T^{-1}), Q is the volumetric discharge (L T^{-3}), A, is the cross-sectional area of the flow face (L^2), and dh/dl is the hydraulic gradient (dimensionless). Following K_{sat}, soil water retention was measured by placing saturated samples in a pressure plate extractor (Soil Moisture Corp. model #1600) on saturated ceramic plates with a 5-bar air entry pressure. Pressure ($|\psi|$) inside the chamber was raised incrementally using the steps 0.1, 1, 5, 10, 20 and 40 m; samples were kept in the chamber at each pressure step for 7 days so mass could stabilize. Between each step, samples were weighed to calculate water content volumetrically (VWC). After the 40 m pressure step, samples were dried in a 105°C oven for 48 hours then weighed to facilitate determination of dry bulk density and porosity.

Soil texture and soil organic matter content (SOM) were determined using the offcuts that remained after subsampling. Clay, silt and sand fractions were measured using a laser scattering particle size distribution analyzer (Horiba Partica LA-950V2) in which the samples were dispersed in a 0.1% sodium hexametaphosphate solution. SOM was determined using the loss on ignition (LOI) method. Before burning, approximately 10 g of each sample was weighed out (in triplicates) and

picked through to remove any twigs or leaves and pulverized to break up any clumps. Samples were left in the muffle furnace for 4 hours at 550°C and re-weighed the following day to determine SOM.

Fine root biomass (FRB) (root diameter < 2 mm) was determined with the core method (Addo-Danso et al., 2016). Each sample was carefully washed through a 2 mm sieve to remove as much soil as possible while minimizing the loss of fine roots. Once washing was complete, the samples were left to air dry and any roots that were easily removed from the remaining soil were separated by hand and set aside. What remained of the samples were then submerged and soaked in a 1% sodium hexametaphosphate solution for four hours. Lastly, roots that were released during the soak were carefully extracted and left to air dry before being combined with roots that had previously been set aside; roots were then weighed to determine FRB (g m^{-2}).

The van Genuchten parameters α, *n*, θ_r and θ_s were estimated using ROSETTA and the RET-C computer code. ROSETTA a computer program that uses five hierarchical pedotransfer functions (PTFs) based on neural network analyses (Schaap et al., 2001). The five PTFs rely on easily obtained soil properties: 1 - soil textural class, 2 - sand, silt and clay fraction (SSC), 3 – SSC plus bulk density (BD), 4 – SSCBD plus water content at field capacity (33 kPa) and 5 – SSCBD33kpa plus water content at permanent wilting point (1,500 kPa). Given the data available, the fourth PTF was used for this analysis. Since *VWC* at 33 kPa was not directly measured during retention experiments, it was estimated using linear interpolation between measured *VWC* values at 10 and 50 kPa.

With the estimated values for α and *n*, field capacity (θ_{fc}) and permanent wilting point (θ_{pwp}) were calculated using equations 2-3 and 2-4:

$$\boldsymbol{\theta_{fc}} = \boldsymbol{n}^{-\mathbf{0.60}\cdot[\mathbf{2}+\boldsymbol{log_{10}}(\boldsymbol{K_{sat}})]} \equiv \frac{\boldsymbol{\theta_{fc}}-\boldsymbol{\theta_r}}{\boldsymbol{\theta_{vG}}-\boldsymbol{\theta_r}} \qquad \textbf{Equation 2-3}$$

$$\boldsymbol{\theta_{pwp}} = \boldsymbol{\theta_r} + \frac{\boldsymbol{\theta_{vG}}-\boldsymbol{\theta_r}}{[\mathbf{1}+(\boldsymbol{\alpha}\cdot\mathbf{1500})^{\boldsymbol{n}}]^{\boldsymbol{m}}} \qquad \textbf{Equation 2-4}$$

where field capacity is defined as the water content corresponding to a drainage rate of 0.1 mm d^{-1} (Twarakavi et al., 2009) and permanent wilting point is defined as water content at 1,500 kPa (Dingman, 2015). With the estimated values for θ_{fc} and θ_{pwp}, available water holding capacity (AWHC) could be calculated as:

$$AWHC = \theta_{fc} - \theta_{pwp}$$ **Equation 2-5**

2.3.1 Statistical methods

All data were tested for normality using a Shapiro-Wilk test; if the test is significant ($p < 0.05$), the null hypothesis that the data is normally distributed can be rejected (Dytham, 2011). For non-normal distributions, a Kruskal-Wallis test followed by a Wilcoxan rank sum post-hoc test was used to determine where, if any, statistically significant ($p < 0.05$) differences occurred between sites. A one-way ANOVA test followed by a Tukey HSD post-hoc test was used for data that were normally distributed. All statistical analyses were conducted using the R Stats Package, version 3.6.1 (R Core Team, 2019).

2.4 Results

2.4.1 Hydrophysical properties

Based on the average sand, silt and clay fractions, soil textural class for each site ranged from sandy loam to clay loam (Table 2-1). Average infiltration rates were lowest at the 6-year site (geometric mean = 93 mm hr^{-1}) and highest at the 9-year site (geometric mean = 857 mm hr^{-1}). Across sites, average infiltration rates initially followed a slight upward trend with time (4 to 8-year), after which values plateaued (Figure 2-2). Significant differences in infiltration rates were detected between the 4-year site and the 6, 8 and 9-year site, and also between the 6-year site and the 8, 9 and-11-year sites. No significant differences were detected between the 7, 8, 9 or 11-year sites. Saturated hydraulic conductivity values were similar to infiltration rates with the largest discrepancy in their geometric means observed at the 6-year site (infiltration rate = 4.2 x 10^{-5} m s^{-1}; K_{sat} = 8.3 x 10^{-5} m s^{-1}). A similar pattern was also observed in K_{sat} values compared to infiltration rates, with a general increase over time; however, there were no significant differences detected between any of the sites (Figure 2-2).

Bulk density followed no apparent trend with time (Figure 2-2). Bulk density of the 7-year site was lowest (0.82 g cm^{-3}) and significantly different than the 4 and 9-year site, while the 6-year site (1.31 g cm^{-3}) was highest and significantly different than the 7, 8 and 11-year sites. There were significant differences detected between values for porosity (θ_s)

Table 2-1 - Average values for LFH properties and vegetation at each site. # of samples = 9 unless otherwise stated. Statistical tests used indicated by: * = Kruskal Wallis and Wilcoxan Rank Sum post-hoc test, ** = one way ANOVA and Tukey HSD post-hoc test.

Property	Years After Reclamation											
	4	**±SD**	**6**	**±SD**	**7**	**±SD**	**8**	**±SD**	**9**	**±SD**	**11**	**±SD**
Infiltration capacity (mm hr^{-1})* (# of samples)	410 (36)	277	93 (106)	432	454 (35)	146	810 (39)	628	857 (41)	864	803 (34)	620
K_{sat} ($m\ s^{-1}$)*	1.2×10^{-4}	4.5×10^{-4}	8.3×10^{-5}	3.4×10^{-4}	1.6×10^{-4}	5.6×10^{-4}	2.4×10^{-4}	1.2×10^{-3}	2.9×10^{-4}	4.5×10^{-4}	2.6×10^{-4}	7.1×10^{-4}
ρ_b ($g\ cm^{-3}$)**	1.14	0.17	1.31	0.23	0.82	0.07	0.88	0.19	1.15	0.28	0.93	0.27
LOI (%)*	8.05	0.02	3.80	0.01	22.86	0.07	9.65	0.04	6.41	0.04	5.31	0.02
Sand (%)**	33	9	51	4	47	6	51	8	34	16	36	9
Silt (%)**	45	6	41	3	40	7	41	8	42	6	39	6
Clay (%)*	21	6	8	2	13	9	7	3	23	14	25	5
Planting Density (SPH)	2431	N/A	1707	N/A	2000	N/A	2471	N/A	2054	N/A	3990	N/A
2018 Density (SPH)	13600	N/A	14400	N/A	47000	N/A	31400	N/A	40400	N/A	17800	N/A
% Increase in Density	459	N/A	472	N/A	1580	N/A	1170	N/A	1866	N/A	346	N/A
Fine Root Biomass ($g\ m^{-2}$) (n = 5)**	28	25	197	56	139	111	251	147	424	243	258	90

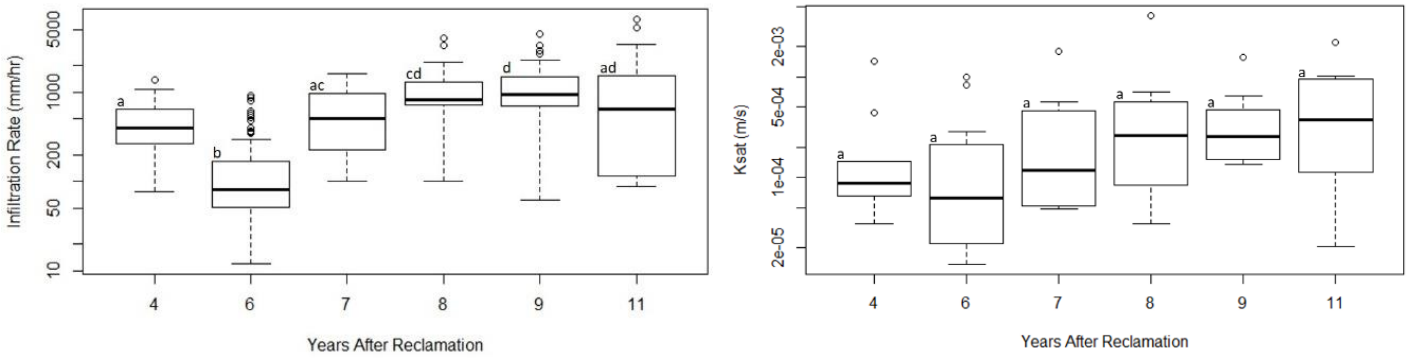

Figure 2-2 - boxplots of infiltration rates and saturated hydraulic conductivity (K_{sat}) for LFH for all sites. Log scale used on y-axis to clarify trends in data. # of samples of samples = 9 for K_{sat}, and varies for infiltration rates - indicated in Table 2-1.

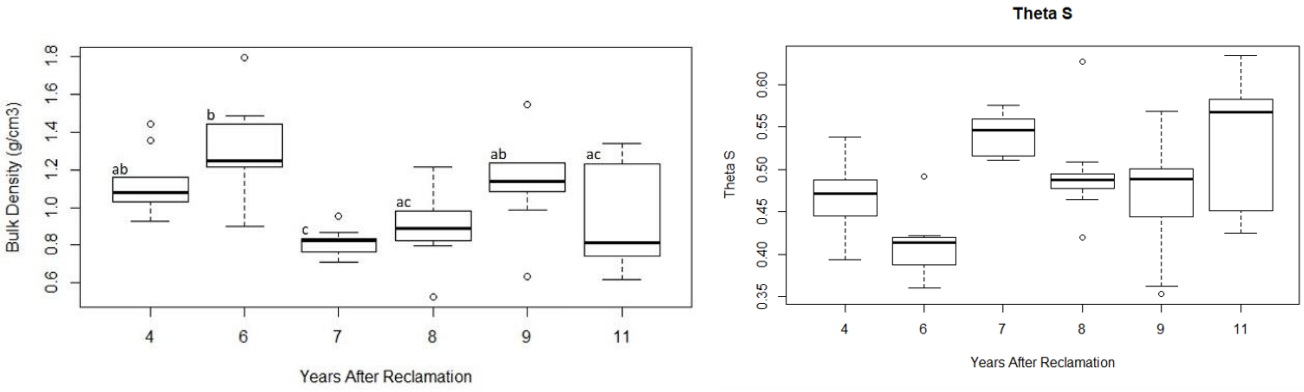

Figure 2-3 - boxplots of bulk density and θ_s of LFH for all sites. # of samples = 9 for each boxplot. θ_s is the values estimated using ROSETTA.

2.4.2 Soil water retention and hydraulic parameter estimation

Table 2-2 presents a comparison of the Van Genuchten parameters α, *n*, θ_s and θ_r, estimated using ROSETTA and RET-C, and Figure 2-4 provides the fit between measured retention data and the continuous SWRC's generated using both sets of parameters. The fit of the measured retention data with RET-C was favourable compared to ROSETTA, which underestimated saturated and residual water content, yet over estimated *VWC* at the 1 m pressure step. Despite the poorer fit using ROSETTA, it provided reasonable α values, and captured the expected increasing trend with time (Benson et al., 2007), that RET-C was unable to do given the absence of data in the critical region governing air-entry (see below), however it is difficult to account for the lack of pattern in RET-C and presence of one with ROSETTA. Differences in *VWC* within the measured soil water retention curves (Figure 2-4) were most pronounced at the 0.1 m pressure step with significant differences detected between the 6 and 11-year sites, and between the 7-year site (*VWC* = 0.65) and all other sites (*VWC* ≤ 0.60). As pressure increased, values for *VWC* remained consistently higher for the 7-year site than all other sites and significant differences were detected between the 7-year site and the 9 and 11-year sites at all pressure steps, and between the 7-year site and the 6-year site at all but the 5 m pressure step. No significant differences were detected between the 4, 6, 8, 9 or 11-year sites.

The van Genuchten parameter α, the inverse of air entry pressure, showed no discernable pattern based on the RET-C analysis (see discussion for explanation), but increased over time according to the ROSETTA approach (Figure 2-5), which produced significant differences between the 11-year site (α = 2.78; lowest air entry pressure) and all others (α ≤ 1.84) except for the 9-year site (α = 2.08). The trend for α was similar to those observed in infiltration rates and K_{sat} (Figure 2-2). Values for *n*, the fitting parameter related to the pore-size distribution, were relatively consistent between sites, regardless of the approach. However, with the exception of the 6-year site, the RET-C values were marginally higher, averaging 1.47, compared to the ROSETTA values that averaged 1.41. Considering the fact that the 6 and 8-year sites had nearly identical sand, silt, clay fractions, yet followed the opposite trends in regards to ROSETTA and RET-C (8-year – ROSETTA was lower than RET-C, 6-year ROSETTA was higher than RET-C), these values are all in a narrow enough range to accept as reasonable.

Values for θ_{fc}, θ_{pwp} and AWHC followed no apparent trend with time and θ_{fc} was relatively consistent between ROSETTA and RET-C, however, θ_{pwp} and AWHC were consistently lower and higher when estimated using ROSETTA, respectively (Table 2-2). Values for AWHC estimated using

ROSETTA were significantly different between the 11-year site and the 6 and 8-year sites and between the 4 and 8-year sites. The only significant differences detected between values for θ_{pwp} were between the 6-year site and all other sites, while values for θ_{fc} revealed significant differences between the 11-year site and the 6 and 8-year sites and between the 6-year site and the 7-year site. Statistical analysis was not performed for the RET-C data.

.

Table 2-2 - Comparison of Van Genuchten parameters and obtained using the ROSETTA PTF and RET C computer code; and θ_{fc} , θ_{pwp} , and AWHC that were calculated using equations 2-3, 2-4 and 2-5, respectively. ROSETTA parameters were obtained by using the average input parameters (SSC, bulk density, *VWC* at 3.3 m) for each site, RET-C parameters were obtained by using the average measured soil water retention curves, number of samples = 9 for each method. Statistical tests used indicated by: * = Kruskal Wallis and Wilcoxan Rank Sum post-hoc test, ** = one way ANOVA and Tukey HSD post-hoc test. No statistical analysis was performed on the RET-C data.

	Parameter	Years After Reclamation											
		4	±SD	6	±SD	7	±SD	8	±SD	9	±SD	11	±SD
ROSETTA	θ_r**	0.06	0.01	0.04	0.01	0.06	0.02	0.04	0.01	0.06	0.02	0.06	0.01
	θ_s*	0.47	0.04	0.40	0.04	0.54	0.02	0.50	0.06	0.47	0.07	0.52	0.08
	α**	1.59	0.83	0.42	0.90	1.29	1.20	1.84	0.72	2.08	0.70	2.78	1.75
	*n**	1.41	0.09	1.49	0.13	1.42	0.14	1.34	0.10	1.42	0.22	1.36	0.11
	θ_{fc}*	0.44	0.03	0.38	0.06	0.44	0.03	0.42	0.04	0.44	0.05	0.47	0.05
	θ_{pwp}*	0.11	0.02	0.08	0.01	0.12	0.03	0.12	0.04	0.12	0.04	0.13	0.04
	AWHC*	0.33	0.01	0.30	0.05	0.32	0.03	0.30	0.01	0.32	0.03	0.35	0.04
	RMSE	0.06	N/A	0.06	N/A	0.09	N/A	0.05	N/A	0.06	N/A	0.04	N/A
	R^2	0.91	N/A	0.91	N/A	0.90	N/A	0.92	N/A	0.93	N/A	0.97	N/A
RET-C	θ_r	0.18	N/A	0.06	N/A	0.23	N/A	0.16	N/A	0.16	N/A	0.20	N/A
	θ_s	0.56	N/A	0.59	N/A	0.69	N/A	0.61	N/A	0.57	N/A	0.62	N/A
	α	8.10	N/A	9.00	N/A	5.33	N/A	8.47	N/A	8.99	N/A	6.27	N/A
	n	1.46	N/A	1.30	N/A	1.57	N/A	1.42	N/A	1.51	N/A	1.56	N/A
	θ_{fc}	0.44	N/A	0.34	N/A	0.45	N/A	0.46	N/A	0.41	N/A	0.45	N/A
	θ_{pwp}	0.19	N/A	0.10	N/A	0.24	N/A	0.18	N/A	0.17	N/A	0.21	N/A
	AWHC	0.25	N/A	0.24	N/A	0.21	N/A	0.28	N/A	0.24	N/A	0.24	N/A
	RMSE	0.01	N/A	0.00	N/A	0.00	N/A	0.01	N/A	0.00	N/A	0.01	N/A
	R^2	0.99	N/A	0.98	N/A	0.99	N/A	0.99	N/A	0.99	N/A	0.99	N/A

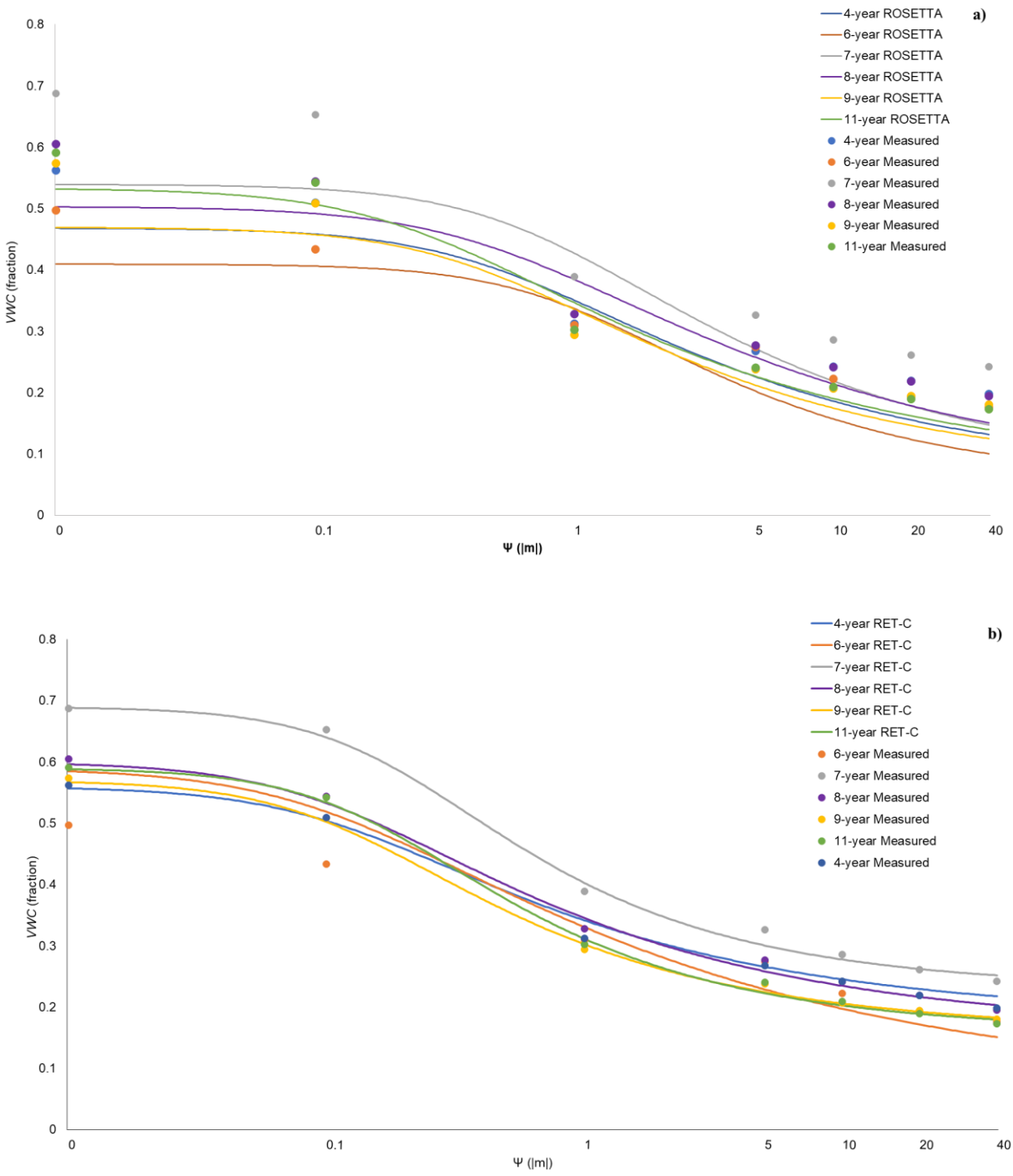

Figure 2-4-Fit of measured retention data with continuous SWRC's generated using α, n, θ_r and θ_s estimated using ROSETTA (a) and RET-C (b). Each curve represents the average of 9 samples.

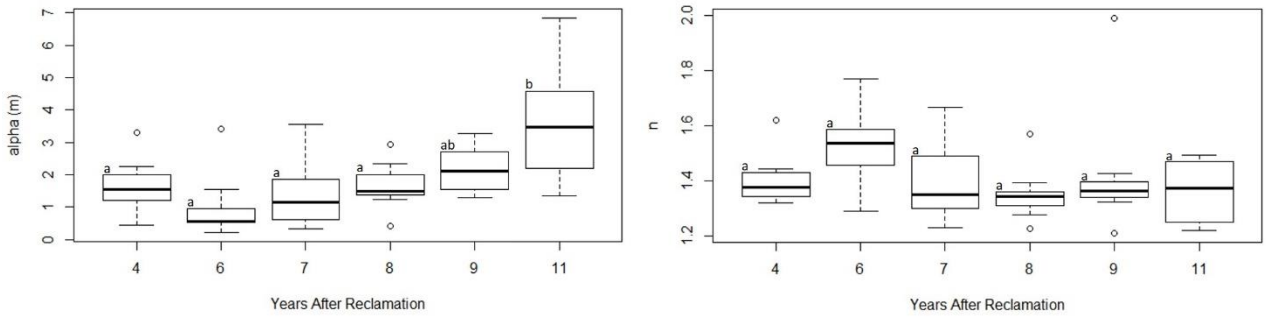

Figure 2-5 - boxplots of van Genucthen α (alpha) and *n* parameters estimated using ROSETTA. # of samples = 9 for all boxplots

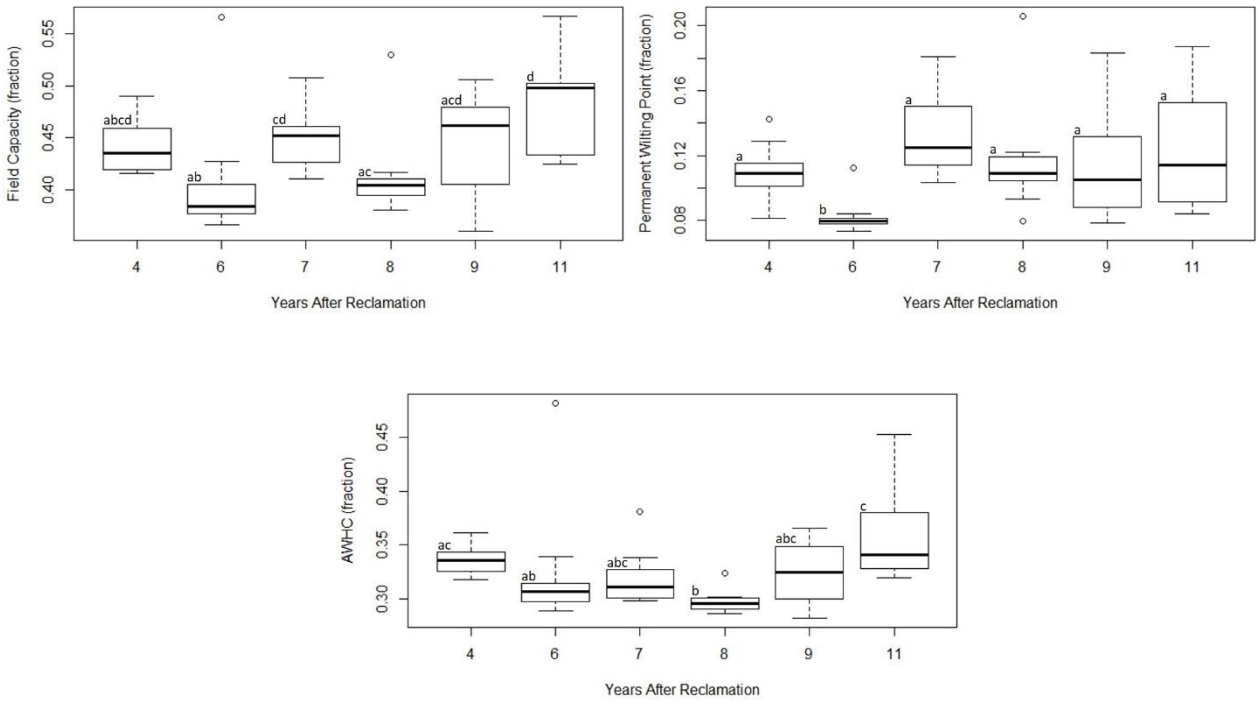

Figure 2-6- boxplots of field capacity, permanent wilting point and available water holding capacity of LFH for all sites calculated using equations 2-3, 2-4 and 2-5, respectively. Values for α and *n* were estimated using ROSETTA. # of samples = 9 for all boxplots.

2.4.3 Site vegetation and soil biological properties

Initial tree planting density varied between sites (Table 2-1), with the lowest initial SPH at the 11-year site (933 SPH) and the highest at the 7-year site (2,797 SPH). Based on the percent increase in density from initial planting to the density measured in 2018 all sites displayed evidence of natural regeneration. The 7-year site had the highest measured 2018 density at 41,600 SPH and the second highest percent increase in density at 1387%. The 9-year site demonstrated the largest percent increase in density from an initial SPH of 2,054 to 36,000 in 2018, which equates to a 1652% increase in density. The 11-year site increased the least (346%) from an initial density of 3990 SPH to a 2018 density of 17,888 SPH.

Soil organic matter content was <10% for all sites except for the 7-year site (~23%), which was significantly higher than all other sites (Figure 2-7). Fine root biomass (FRB) demonstrated an upward trend over time (Figure 2-7) from the 4-year site (28 g m^{-2}) to the 9-year site (424 g m^{-2}); however, the 11-year site diverged from this trend with average values similar to the 7-year site. Statistical analysis reflects the trend with age as significant differences were detected between the older (9-year) site and younger (4 and 6-year) sites.

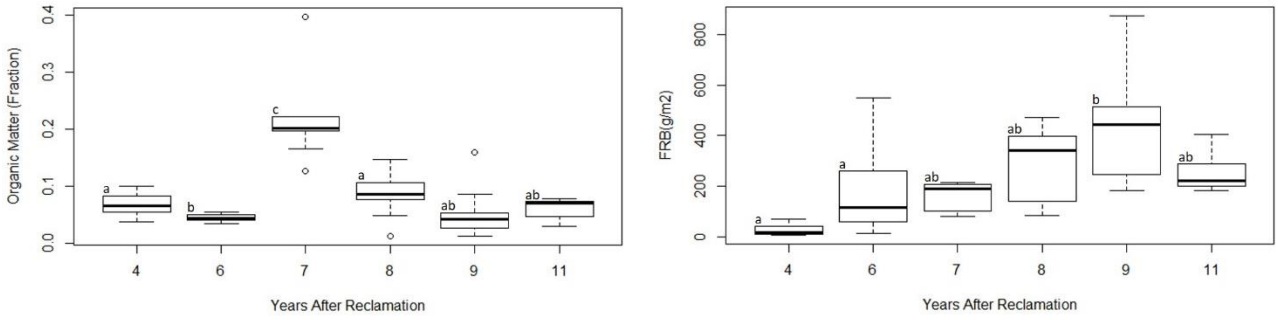

Figure 2-7 - boxplots of soil organic matter and fine root biomass for LFH from all sites. # of samples = 9 for all boxplots.

2.5 Discussion

2.5.1 ROSETTA vs RET-C

Discrepancies were noted between α, θ_r and θ_s estimated using ROSETTA and RET-C (Table 2-2). In particular, α was consistently higher with RET-C than with ROSETTA. This may be due to the fact that the measured retention data (input for RET-C) was lacking pressure steps at the "wetter" end of the SWRC and thus the actual air entry pressure, which is approximated by α, was likely missed. The higher values for α estimated using RET-C (5.3 – 8.9 1 m^{-1}) would equate to higher values (less negative) for air-entry pressure than the lower values for α provided by ROSETTA (0.94 – 3.54 1 m^{-1}). Considering the gap in data for the portion of the measured retention curve that would capture air entry, RET-C likely estimated air-entry based on the first pressure step (-0.1 m), while ROSETTA was able to consider a wider range of pressures. The fact that ROSETTA values for α followed the expected increasing trend with time, while those estimated using RET-C did not, is more difficult to account for. Since the input data used for ROSETTA revealed no trend with time as individual properties (SSC, bulk density, *VWC* at field capacity), the differences in patterns may be attributed to the way ROSETTA works. ROSETTA uses artificial neural network analysis that uses the optimal and variable relations that link input data to output data (Schaap et al., 2001); unlike other pedotransfer functions that apply a series of linear or non-linear regression equations to input data (Minasny et al., 1999) and are thus more readily available to the user for inspection.

Values for θ_s estimated using ROSETTA were consistently lower than those estimated using RET-C, and align well with typical values for loam (predominant soil type in this study) (Dingman, 2015), however ROSETTA is unable to account for soil structure (*e.g.* larger pores). This could cause a discrepancy in values since θ_s estimated using RET-C is provided by the input value of saturated water content that in this case was measured in the laboratory, and thus captures the presence of larger pores that are filled with water at saturation, yet may not impact bulk density to the degree that it would alter a result from ROSETTA. The poor match between values for θ_r, which was consistently much lower for ROSETTA than it was for RET-C, may be attributed to the insufficiently low pressures in the input data to obtain a true value for θ_r with RET-C. Residual water content is often defined as *VWC* at -150 m, the lowest pressure that can typically be measured in the laboratory (van Genuchten, 1980), however the input data for RET-C did not include values for *VWC* at

pressures lower than -40 m. The θ_r values provided by RET-C are a close match to measured *VWC* values at -40 m (Figure 3-2, Table 2-2), suggesting that the range of pressures in the input data was too narrow and RET-C was unable to extrapolate to lower pressures associated with residual water content (similar to the lack of data in the air-entry range). The lower values for θ_r estimated using ROSETTA can be attributed to the fact that ROSETTA employs a database of measured retention data, and can thus link known input parameters (SSC, bulk density, *VWC* at -3.3 m) to similar soils that have known values for *VWC* at -150 m (Schaap et al., 2001).

The relatively good match between ROSETTA and RET-C for θ_{fc} (Table 2-2) can also be attributed to the input data used for each method. ROSETTA used *VWC* at -3.3 m, which was estimated by linear interpolation between the values for *VWC* measured at -1 m and -5 m. This suggests that, despite the lack of data at -3.3 m for the RET-C input, it was able to capture this missing portion of the SWRC, unlike more critical portions, such as air-entry pressure. Since θ_{pwp} is also defined as *VWC* at -150 m (van Genuchten, 1980), the poor match between ROSETTA and RET-C can be linked to the poor match between values for θ_r. Finally, the differences between AWHC estimated using each method are a result of θ_{pwp} since AWHC = θ_{fc} - θ_{pwp}.

2.5.2 Evolution of soil properties

The goal of this study was to determine the extent to which LFH mineral mix cover soil evolves post-placement. Given that all sites' average soil textural classification was loam, a space-for-time analogy was used to make comparisons between sites and comment on trends over time. The assumption is that similar textural classifications should react similarly over time to biotic and abiotic forces that influence a soil's development. While there were some general trends, such as increasing infiltration rate with age (Figure 2-1) and a similar pattern for α, distinct differences in structural properties, such as bulk density or texture had a strong influence that superseded an age effect. For example, the 6-year site had the highest bulk density (Figure 2-2) and lowest SOM of all sites (Table 2-1), and its infiltration rate (Figure 2-1) was lowest, even though its clay content (Table 2-1) was amongst the least. By comparison, at the 4-year site, the bulk density and SOM were relatively high, and was associated with higher infiltration rates than the older 6-year site, even though the former had much higher clay content. The complexity of the interrelationships between soil properties, irrespective of

time, are highlighted in the correlation matrix (Figure 2-8), which will be referenced throughout the discussion.

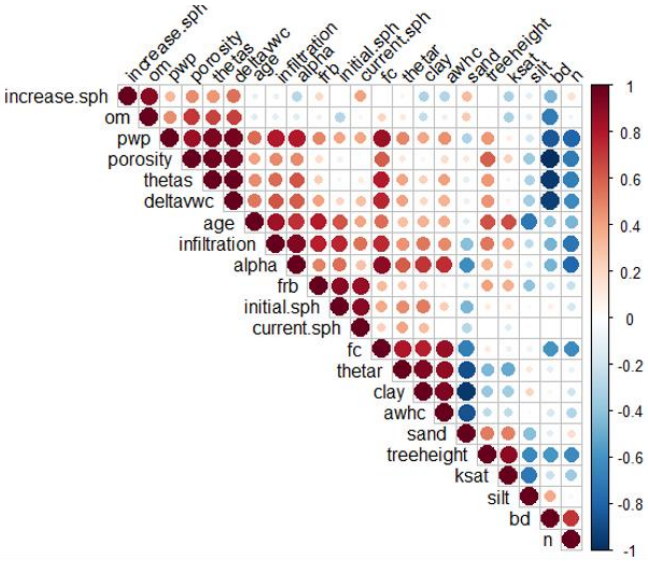

Correlation matrix	In text
increase.sph	% Increase in Density
om	SOM
pwp	θ_{pwp}
porosity	φ (fraction)
thetas	θ_s
deltavwc	Δ VWC
age	Years since reclamation
infiltration	Infiltration (mm hr^{-1})
alpha	α
frb	FRB (g m^{-2})
initial sph	Planting density
current sph	2018 density
fc	θ_{fc}
thetar	θ_r
clay	Clay (%)
awhc	AWHC
sand	Sand (%)
treeheight	Tree height (cm)
ksat	K_{sat} (m s^{-1})
silt	Silt (%)
bd	ρ_b (g cm^{-3})
n	n

Figure 2-8 - correlation matrix generated using R illustrating relationships between all variables. Red indicates a positive correlation and blue indicates a negative correlation. Strength of relationship indicated by size and shade of symbol (*e.g.* smaller and lighter denotes a weaker relationship). The table to the right clarifies discrepancies in how variables were named in the figure and throughout the text.

With respect to infiltration rates, the presence of a slight upward trend with time (4 - 9-year), suggests that while biotic processes continue to condition the soil, it is likely that infiltration rates had already begun to plateau, even at the 4-year site. This supports findings by others that in reclamation soils, hydraulic conductivity and infiltration rates plateaued 2-4 years following placement (Benson et al., 2007; Kelln et al., 2007; Guebert Gardner, 2001; Meiers et al., 2011). Changes to infiltration rates in reclaimed soils have been attributed to freeze-thaw cycling (Benson et al., 2007) and laboratory experiments on compacted clays demonstrated a reduction in the effect of freeze-thaw cycling (FTC) on hydraulic conductivity after 2-4 FTCs (Benson, 1992). In this study, the weak trend of increasing

infiltration capacity with time, is for the period after which most change is normally anticipated (Benson et al., 2007; Kelln et al., 2007; Guebert and Gardner, 2001; Meiers et al., 2011). Further, Sutton and Price (2019) demonstrated that freeze-thaw cycling of LFH in the first few years following placement at the Nikanotee Fen Watershed (6-year site) weakened the capillary barrier that restricted recharge from LFH to tailings sand. Average infiltration rates at the 8, 9 and 11-year sites are approaching those measured in 2015 at a nearby natural site (Elmes and Price, 2019), where average infiltration rates were 1011 mm hr^{-1} and soil textural classifications (sandy loam, loam and clay loam) were similar to those found in this study.

The data provides evidence that other processes continue to alter the structure of LFH in later years of reclamation. The upward trend with time noted in the van Genucthen parameter α (1.79 – 3.54; Figure 2-4) indicates a decrease in air-entry pressures and thus the presence of larger pores. Benson et al. (2007) noted an increase in α by up to a factor of 10 for soils with very small as-built values (very high air entry pressure), 2-4 years post-placement. The magnitude of change diminished with higher as-built values for α. Similarly, Sutton and Price (2019) noted an increase in α from 1.3 to 5.8 between unweathered and weathered LFH, respectively, at the NFW (6-year site). Further indication of the continual development of larger pores in LFH is evidenced by the upward trend with time noted in maximum infiltration rates (i.e. outliers on Figure 2-2). Mechanisms that may be responsible for the development of larger pores in the timeframe of this study (4 - 11-years) include soil macrofauna (Weiler and Naef, 2003) and the proliferation of plant roots that drive soil aggregation and thus improve structure (Scholl et al., 2014). Improved soil structure results in larger pores as soil particles are either pushed together by the force of roots or are held together by the mycelium of mycorrhizal fungi, creating voids between the newly formed aggregates (Rillig and Mummey, 2006). The increased presence of fine roots can be seen in the upward trend with time noted in fine root biomass (FRB) as well as its relationship with site age (R^2 = 0.78; Figure 2-8). The continued development of larger pores suggests that LFH's hydrologic response will improve with time. In a comparison of two slopes reclaimed using PMM in 2007 and 2011, Ketcheson and Price (2016) found that the younger slope produced surface runoff far more frequently than the older slope, attributing the differences in hydrologic response between slope to differences in their hydrophysical properties.

Other properties presented did not follow any distinct trends over time or remained consistent between sites. For instance, the highest and lowest values for bulk density were detected at the 6 and 7-year sites, respectively. Bulk density did, however, present strong negative relationships with

certain soil water retention parameters (Figure 2-8). The relationship between bulk density and the van Genuchten parameter θ_s and the measured change in storage between the 0.1 m and 40 m pressure steps have an R^2 of -0.96 and -0.94, respectively. Given that the measured and van Genuchten soil-water retention curves (Figure 2-3) follow no obvious trend with time, it is likely that bulk density has a strong control on soil-water retention in LFH. Further, since bulk density was not correlated with years since reclamation; it is likely an intrinsic property of the soil at placement. Conversely, AWHC and bulk density have a weak relationship (R^2 = -0.17; Figure 3-1), illustrating the differences between soil-water retention and AWHC. Soil-water retention is a measure of how much water a soil will physically hold onto under varying pressure heads, while AWHC is a parameter that estimates the amount of water available to plants, between two distinct points on the soil-water retention curve (Equation 2-5). AWHC is controlled by soil texture as demonstrated by the relationship between AWHC and clay fraction (R^2 = 0.93) and sand fraction (R^2 = -0.87).

In addition to following no trend with time, bulk density measured in this study differs substantially from bulk density measured at natural sites. The soil at the natural site previously mentioned had an average bulk density of 0.37 g cm^{-3} (Elmes and Price, 2018), less than half of the lowest bulk density in this study, measured at the 7-year site (0.82 g cm^{-3}). Despite this, average bulk density values for all study sites do not exceed the range at which bulk density may restrict root growth (1.6 g m^{-3}; Houlbrooke et al., 2010), including the 6-year site which was the only site to receive stockpiled LFH.

Comparison of results from the Nikanotee Fen Watershed

A set of samples were collected from the 6-year site (Nikanotee Fen Watershed) in 2013 (equivalent to year 1) and similar soil physical properties were previously measured. Table 2-3 presents a comparison of results between 2013 and 2018. While there were no significant differences detected between any of the properties (sample numbers were low, but many properties had similar values), some did exhibit patterns worth noting. Infiltration capacity more than doubled from 41 mm hr^{-1} to 93 mm hr^{-1} (p = 0.14), while α increased from 0.50 to 0.94 (p = 0.2) and n decreased from 1.61 to 1.52 (p = 0.2). The patterns in α and n point to a greater presence of larger pores and a broadening of the pore-size distribution (Benson et al., 2007; Sutton and Price, 2019). These results further support the idea that the mechanisms that contribute to a soil's evolution change with time since placement (short term, abiotic; long term, biotic). Over a longer time-frame, changes to bulk density and SOM may occur that could influence soil-water retention. Additionally, the 6-year site was the only one to

receive stockpiled LFH (i.e. presumed to be of lower quality), and although there was a substantial increase in infiltration capacity since 2013 (Table 2-2), the 2018 average infiltration rate was still significantly lower ($p < 0.001$) than the youngest site in this study (4-year), and its bulk density was highest (Table 2-1). These data are consistent with the current best-management practices for reclamation that favour directly placed LFH over stockpiled LFH (Mackenzie, 2011; Naeth et al., 2013).

Table 2-3- Comparison of results from Nikanotee Fen Watershed. Infiltration capacity, bulk density and porosity are from Ketcheson (2015) and SOM is unpublished data (Ketcheson, 2013). θ_r, θ_s, α and n were estimated using ROSETTA and those results were used to calculate θ_{fc}, θ_{pwp} and AWHC.

Year	Infiltration capacity (mm hr^{-1})	ρb (g cm^{-3})	Porosity (cm^3/cm^3)	θ_r	θ_s	α	n	θ_{fc}	θ_{pwp}	AWHC	SOM (%)
2013 $n = 7$	41	1.30	0.45	0.05	0.40	0.50	1.61	0.38	0.07	0.30	4.56
2018 $n = 9$	93	1.31	0.51	0.05	0.41	0.94	1.52	0.40	0.08	0.32	4.40

2.5.3 Initial quality

SOM may be used as an indicator of quality for reclamation soils given its role in soil fertility and ecosystem functioning (Turcotte et al., 2009). Based on SOM, there is evidence that initial quality of LFH at time of placement differed between sites, as illustrated by the 7-year site. SOM at the 7-year site (23%) was more than 2 x greater than all other sites. Since natural changes to SOM typically take place over longer periods of time than this study covers (Bradshaw, 1997), it is reasonable to attribute this substantial difference in SOM to the LFH's place of origin or salvage depth, which can result in a salvaged material with an inherently different fraction of organic matter. In support of this, Macyk (2006) found natural layers of LFH in the AOSR to range from 2– 25 cm, depending on location. Higher SOM is linked to lower bulk density (Dexter, 2004) and higher soil water retention (Yang et al., 2014), which is reflected by the 7-year site where bulk density was the lowest and measured soil-water retention the highest. Additionally, the 7-year site displayed the second highest level of natural canopy regeneration based on percent increase in density from time of planting to 2018.

Despite evidence that higher initial quality seems to instigate "quicker" success in reclamation, sites with lower quality LFH still display signs of successful reclamation, as

demonstrated by the 6 and 11-year sites. The 6-year site had the lowest average infiltration rate (92 mm hr^{-1}), highest bulk density (1.3 g m^{-3}), and lowest SOM (3.8%). The 11-year site had the second lowest SOM (5.3%) and lowest amount of natural regeneration (346%). These were also the only two sites that required additional fill-in planting one or two years after initial planting due to seedling mortality. Additionally, the 6-year site was the only one to receive stockpiled LFH rather than direct placement, the preferred method, as propagules in stockpiled LFH have been shown to lose viability (Naeth et al., 2013). Although both sites exhibit poorer individual properties relative to the other study sites, they have both developed into functional uplands that support the continued establishment and growth of vegetation.

2.5.4 Limitations

Although this study used relatively simple methods to obtain a set of well understood soil hydrophysical properties, limitations of the study design and approach should be noted. For instance, the use of space-for-time to characterize the evolution of a landscape must be considered in the application of these results. While each study site employed similar techniques in reclamation (*e.g.* cover crop, fertilizer application, time of placement and planting), and were all similar in texture, variability in their places of origin impacted certain properties. As a result, it is difficult to obtain a baseline from which those properties can be tracked without carrying out a multi-year study on the same study site. Additionally, the time frame of the study (4 – 11 years post reclamation), is relatively narrow and thus any longer-term changes to soil structure and quality could not be captured.

Another limitation of a study that uses space for time, is that the assumption of similarity in materials does not account for differences in outside forces such as soil placement depth, weather conditions from year to year, or soil properties that are especially sensitive to abiotic forces. For instance, the differences in clay content in each LFH could have an impact on the way LFH reacts to freeze-thaw cycling; soils with a high clay content would be more readily altered as a result of FTC. Additionally, since each site was constructed in a different year, they were exposed to different weather patterns, so even if they were similar in regards to materials used, the forces acting on those materials differ. Finally, since the ROSETTA PTF relies on some input properties that will not change with time (sand, silt, clay fractions), its ability to capture a trend in α, n, θ_r and θ_s rests on a change in *VWC* at 3.3 m and bulk density (and 150 m if applicable); and thus this method may be insufficient for studies that use space for time to assess the evolution of soils.

2.6 Conclusion

The use of six spatially and temporally distinct study sites captured the variability in LFH mineral mix and highlighted the complexity of relationships between soil physical properties. Despite its variability, the current study revealed LFH used at the respective study sites can support the intended cover-soil function, including recharge in the upland of an upland-fen watershed. Although most of the study sites investigated were built in a manner that could restrict percolation (*e.g.* overburden dump and tailings sand dikes), the properties presented were measured in the upper 10 cm of soil and can therefore be considered under a different context where percolation is not restricted.

LFH can support the establishment and growth of vegetation and perform hydrologically in a way that promotes recharge. The continued growth and establishment of vegetation with time, as evidenced by tree height, FRB, and percent increase in density, contributes to the alteration of the soil's structure once the effect of abiotic forces, such as freeze-thaw cycling, has diminished. Further, AWHC measured at all sites (0.3 – 0.35), which represents water available to plants, exceeds AWHC measured in natural soils in the AOSR (~0.1) (Macyk, 2006). The increasing trend with time noted in α and maximum infiltration rates points to the continual development of larger pores within the soil matrix, contributing to an improved hydrologic response and thus a greater ability to transmit water into the subsurface via macropore flow (Beven and Germann, 1982; Weiler and Naef, 2003).

Since properties such as bulk density and SOM followed no trend with time it is likely that they are an intrinsic property of LFH upon placement and contribute to its initial quality. Higher initial quality does seem to contribute to quicker success in reclamation, as evidenced by the 7-year site where SOM was significantly higher than all other sites and demonstrated the second highest amount of natural regeneration. However, sites that received LFH of lower initial quality (6 and 11-year), still functioned as intended, despite issues with seedling mortality in the earliest years of reclamation. A comparison of year 1 data to year 6 data from the NFW (6-year site) reinforces the idea that properties such as bulk density are an intrinsic property upon placement. While it is possible that changes to bulk density may take place over longer time frames as biotic forces continue to alter a soil's structure, this was not captured by the timeframe this study.

The dynamic nature of certain properties in LFH mineral mix (*e.g.* infiltration capacity and α) support the use of LFH of lower quality at time of placement, including LFH that was stockpiled. If care is taken through the use of industry established best practices, the hydrophysical quality of LFH should improve with time and the continued establishment and growth of vegetation, once the influence of abiotic forces such as freeze-thaw cycling has diminished. These changes will contribute

to an upland cover soil that is able to support vegetation and promote recharge into the subsurface, two qualities that are necessary for success in the upland of an upland-fen watershed.

Considering the comparison of results obtained using RET-C and ROSETTA for the van Genuchten parameters α, *n*, θ_r and θ_s as well as θ_{fc} and θ_{pwp} and AWHC, a more robust analysis of ROSETTA to analyze soils used in reclamation is warranted. While there were discrepancies between methods, a more in-depth study could provide greater clarity to those differences and potentially support the use of ROSETTA in the future, allowing for the quick analysis of spatially robust data to characterize materials used in land reclamation in the AOSR.

Chapter 3
Implications of LFH mineral mix in a layered soil profile

3.1 Introduction

Resource extraction activities in the Athabasca Oil Sands Region (AOSR) results in the complete removal of the uplands and peatlands, which are characteristic of the region (Rooney et al., 2012). These landscapes provide essential ecosystem services and are crucial to the hydrological functioning of the area (Devito et al., 2012). Through land reclamation, the Government of Alberta requires that disturbed lands be returned to an equivalent land capability (Alberta Environment, 2010). Successful reclamation requires an understanding of the physical, chemical, and biological properties of salvage materials and the impact they have on intended landscape function. Common salvage materials incorporated into the reclamation landscape include overburden and tailings sand, used to construct upland landforms and dikes, cover soils salvaged from the pre-mined landscape, and subsoils typically composed of glacial till, to act as a buffer between the two (Mackenzie, 2011). In addition to understanding these materials individually, it is necessary to consider the interactions between soils in a layered profile. When layered, barriers to percolation may occur as a result of the contrasting hydraulic properties of the materials used, impacting the hydrological functioning of a reclaimed landscape (Huang et al., 2013; Leatherdale et al., 2012; Naeth et al., 2011).

Reclamation landscapes that are built with the intention of supporting upland boreal vegetation and limiting the movement of contaminants in the subsurface (*e.g.* saline sodic overburden dumps or tailings sand dikes) benefit from the presence of a percolation barrier (Kelln et al., 2007). In layered profiles, field capacity in the cover soil can be increased, thereby increasing available water holding capacity (AWHC), resulting in improved soil water storage in the rooting zone compared to a homogeneous profile (Huang et al., 2013). This is beneficial to vegetation in the AOSR where the climate is characterized by short, intense precipitation events that are separated by longer periods when little to no precipitation occurs and vegetation may become water stressed (Devito et al., 2012). More recent efforts in reclamation research include the construction of an upland-fen watershed. In contrast to an overburden dump, an upland-fen watershed must maintain hydrological connectivity between its upland cover soil and underlying aquifer to promote groundwater recharge, yet still maintain soil water storage in the rooting zone sufficient for the establishment and growth of vegetation (Sutton and Price, 2020; Ketcheson et al., 2017; Price et al., 2010).

The nature of percolation barriers created by layering reclamation materials depends on the arrangement in relation to their hydraulic properties. For instance, when a finer soil is placed over a coarser soil, a capillary barrier may be formed. Under unsaturated conditions, the coarser underlying soil will remain less permeable relative to the overlying finer (hence more saturated) soil, limiting the movement of water across the interface (Yang at al., 2004; Sutton and Price, 2019). Water held above the interface of the two soils will be removed from the finer soil by evapotranspiration, or breakthrough when the capillary barrier is broken, releasing water into the underlying soil (Stormont and Anderson, 1999; Yang et al., 2004). Breakthrough occurs when soil-water pressure at the interface is increased to the breakthrough head (ψ_B) of the coarser soil. Breakthrough head is the lowest pressure at which larger amounts of water could enter the coarser soil and can be identified by the inflection point of the soil water retention curve (SWRC), which corresponds to a rapid increase in permeability (Hillel and Baker, 1988; Stormont and Anderson, 1999). Therefore, by determining the point of the finer soil's SWRC that corresponds to the breakthrough head of the coarser soil, it is possible to estimate the *VWC* needed in the finer soil for breakthrough to occur (Khire et al., 2000). In the case of a coarse soil placed over a fine soil, a hydraulic barrier may be created by contrasting hydraulic conductivities. If the overlying coarser soil has a higher hydraulic conductivity than the underlying soil, water moving through it will be slowed down at the interface of the two soils and thus be held closer to the surface for a greater duration (Li et al., 2014).

The impact that percolation barriers have on the hydrological functioning of reclaimed landscapes has been discussed in the literature. Naeth et al. (2011) noted a capillary barrier at a tailings sand storage facility that had been directly capped with peat-mineral mix (PMM). The capillary barrier persisted throughout most of the growing season, as evidenced by water contents in the PMM, which remained close to field capacity; when field capacity was surpassed the capillary barrier was broken through and an increase in *VWC* was observed below the PMM – tailings sand interface. Similar observations were made by Leatherdale et al. (2012) in reclamation landscapes capped with PMM overlying both tailings sand and subsoil (*e.g.* glacial till). They concluded that the presence of the capillary barriers were a benefit to the way the systems functioned as a result of enhanced soil-water retention. Conversely, at another site in the same study, Leatherdale et al. (2012) noted water contents in PMM overlying tailings sand that consistently fell below permanent wilting point throughout the growing season, illustrating the variability in these systems and the materials used to construct them. In the upland of an upland-fen watershed, Sutton and Price (2019) identified a capillary barrier at the interface of LFH overlying tailings sand. Given the unique goals of an upland-

fen watershed, the presence of a capillary barrier could negatively impact the functionality of the landscape as its adjacent fen relies on groundwater inputs from the tailings sand aquifer (Ketcheson et al., 2017). Although reclamation landscapes may differ in intended function, out of necessity they employ similar materials in their construction to achieve these different results. A greater understanding of the implication that cover soils and their interactions with subsoils have on the intended performance of a system is necessary for future design decisions. While field studies, such as those discussed above, are necessary for making observations in a natural setting subject to natural variability, laboratory studies provide the opportunity to make observations where certain variables can be controlled; thus, making comparisons across different sites more reliable. Laboratory column experiments are a valuable tool to study the movement of water through a layered soil profile. Specifically, monolithic samples offer an opportunity to closely mimic field conditions since soil physical properties that influence hydrological processes remain relatively undisturbed (Kosugi, 2002; Lewis and Sjöstrom, 2010).

The focus of this research will be the use of LFH-mineral mix in layered soil profiles in reclamation landscapes. Laboratory column experiments will be employed to observe the movement of water through three temporally and spatially distinct profiles capped with LFH. The specific objectives are to 1) assess the implications of a percolation barrier at an LFH-subsoil interface, depending on landscape function, and 2) assess the applicability of laboratory based data in determining if a barrier exists, and what kind of barrier could be expected.

3.2 Study sites

Soil monoliths were extracted from three reclamation study sites, to assess the influence that LFH mineral mix (hereafter referred to as LFH) has on groundwater recharge. The sites, located approximately 30 km north of Fort McMurray, Alberta (56°55’52”N, 111°24’59”W) were all capped with a layer of LFH at the time of reclamation (2007, 2010 and 2012). Years since reclamation at the time of sampling (May - August 2018) will be used to refer to each site (11-year, 8-year, 6-year). The 8 and 11-year sites were overburden dumps constructed using saline sodic overburden, covered with 100 cm of subsoil (glacial till) prior to being capped with a 20 cm layer of LFH. The 6-year site was the upland of a constructed upland – fen watershed (Nikanotee Fen Watershed). Tailings sand used to create the aquifer that forms the upland was capped with approximately 30 cm of LFH in the upland portion of the landscape.

3.3 Methods

3.3.1 Laboratory column experiments

One 30 cm I.D x 45 cm length monolith was collected from a random location at each of the three study sites. The thickness of 45 cm was chosen to ensure each sample would capture the interface between the LFH and its subsoil, therefore each monolith contains a layer of each material. The samples were collected in a manner that caused minimal disturbance and not require further manipulation once in the laboratory. To achieve this an access trench approximately 50 cm deep was dug adjacent to the location from which the monolith was taken; then, a pre-cut length of PVC conduit was placed upright on the ground next to the trench. Using hand trowels the sample was carefully extracted by digging downward around the outside of the tube and removing enough material along the sides so that the tube could be pushed down yet leave minimal space between it and the soil. This was done approximately 5 cm at a time until the top of the tube was flush with the ground. To remove the monolith a stiff metal plate was placed on the bottom of the trench and carefully wedged beneath the sample, cutting it off at the base. Next, the sample was lifted out of the trench and closed on both ends using plastic caps secured using vapor proof tape. Before backfilling the extraction site, one intact 10 cm x 10 cm sample of the subsoil was collected at the 8 and 11-year sites from the wall of the hole left after extracting the monolith, approximately 5 cm below the LFH-subsoil interface. A subsoil sample was not collected at the 6-year site, however work on the same site (Ketcheson, 2015) provided values for certain properties of the tailings sand, and the ROSETTA pedotransfer function (discussed in the following section) was used to estimate saturated hydraulic conductivity. The monoliths were stored at room temperature until they could be transported back to the University of Waterloo. All samples were secured and wrapped to minimize disturbances caused by transport. An additional nine intact LFH samples (10 cm I.D x 10 cm height) were collected from random locations at each site to characterize the average LFH properties.

Laboratory column experiments were employed to observe the movement of water through LFH and into its underlying material. To irrigate the monolith, water was applied using Tygon^{TM} tubing (3/4" I.D), spiraled and affixed to a circular plate that was mounted above the monoliths. Small holes were drilled in the tubing every 5 cm for a total of 25 holes through which water could drip. Deionized water was supplied to each irrigation apparatus using a peristaltic pump (Longer Pump WT600-3J) at a rate of 60 rotations per minute (rpms) resulting in an irrigation rate equivalent to 57.5 mL minute^{-1}, or 3,450 mL hour^{-1}. Three irrigation events over the course of three days were carried

out as follows: irrigation event #1 - 1 hour, 3,450 mL, irrigation event #2 - 2 hours, 6,900 mL, irrigation event #3 - 3 hours, 10,350 mL. Between each irrigation event and at the end of the experiment the monoliths were covered with a layer of polyethylene film to prevent evaporation. No water was applied to the monoliths prior to the beginning of first irrigation event and thus the experiment was conducted with the monoliths in the condition they were collected in the field. Soil moisture within each monolith was measured using four Campbell Scientific CS605 probes placed 2.5 cm below ground surface (bgs), 3 cm above and 3 cm below the LFH – subsoil interface and 35 cm bgs. The probes were connected to a multiplexer (Campbell Scientific SDMX50) and Time Domain Reflectometer (Campbell Scientific TDR 100) and data were logged every 15 minutes using a Campbell Scientific CR1000 data logger. The monoliths were placed on a 4.5 cm bed of glass beads (diameter 75 – 95 µm, K_{sat} = 5 x 10^{-5} m s^{-1}) that were kept saturated using a Marriot bottle by setting the water table at the interface of the subsoil and glass beads, 4.5 cm above the base (Figure 1-1). Outflow was measured using a tipping bucket rain gauge (Texas Electronics TR-525M), placed beneath the outlet of each monolith. Data from the tipping buckets were logged every 15 minutes on the same data logger as the TDR probes.

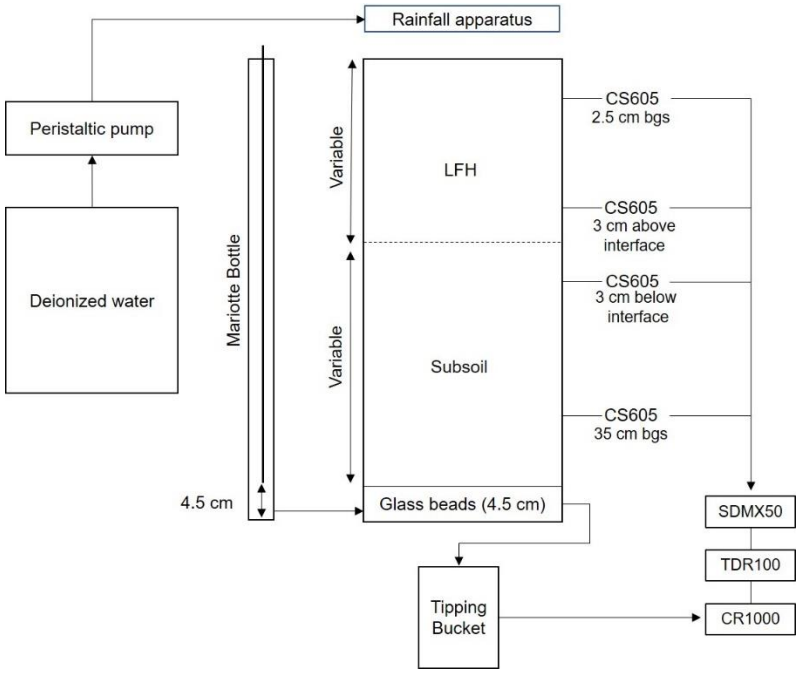

Figure 3-1 - Schematic diagram of laboratory column experiments.

3.3.2 Soil physical properties

Intact cores were sub-sampled in the laboratory using stainless steel rings to produce smaller intact cores (8 cm I.D x 5 cm height), with the leftover sample stored separately. The smaller intact cores were used to measure saturated hydraulic conductivity (K_{sat}), soil water retention, bulk density and porosity. K_{sat} was measured using the KSAT System (Meter Group) falling head method. Following K_{sat}, soil water retention was measured by placing saturated samples in a pressure plate extractor (Soil Moisture Corp. model #1600) on saturated ceramic plates with a 5-bar air entry pressure. Pressure ($|\psi|$) inside the chamber was raised incrementally using the steps 0.1, 1, 5, 10, 20 and 40 m; samples were kept in the chamber at each pressure step for 7 days so mass could stabilize. Between each step, samples were weighed to calculate water content volumetrically (*VWC*). After the 40 m pressure step, samples were dried in a 105°C oven for 48 hours then weighed to facilitate determination of dry bulk density and porosity. With the offcuts that remained after subsampling, clay, silt and sand fractions were measured using a laser scattering particle size distribution analyzer (Horiba Partica LA-950V2) in which the samples were dispersed in a 0.1% sodium hexametaphosphate solution. Since no subsoil sample was collected from the 6-year site, values for sand, silt and clay fractions, as well as bulk density and porosity were obtained from Ketcheson (2015), in which the 6-year site (Nikanotee Fen Watershed) was characterized. K_{sat} was estimated using the ROSETTA pedotransfer function, discussed below.

The van Genuchten parameters α, *n*, θ_r and θ_s were estimated using ROSETTA, a computer program that uses five hierarchical pedotransfer functions (PTFs) based on neural network analyses (Schaap et al., 2001). The five PTFs rely on easily obtained soil properties: 1 - soil textural class, 2 - sand, silt and clay fraction (SSC), 3 – SSC plus bulk density (BD), 4 – SSCBD plus water content at field capacity (33 kPa) and 5 – SSCBD33kpa plus water content at permanent wilting point (1,500 kPa). Given the data available, the fourth PTF was used for this analysis. Since *VWC* at 33 kPa was not directly measured during retention experiments, it was estimated using linear interpolation between measured *VWC* values at 10 and 50 kPa. For the 6-year site tailings sand, the third PTF was used since measured retention data were not available to estimate *VWC* at 33 kPa. With the estimated values for α, *n*, θ_r and θ_s, soil water retention curves (SWRC) and hydraulic conductivity curves were generated using equations 3-1 and 3-2 (van Genuchten, 1980):

$$\boldsymbol{\psi(\theta) = \theta_r + (\theta_s - \theta_r)[1 + (\alpha\psi)^n]^m} \qquad \textbf{Equation 3-1}$$

$$K(\theta) = K_s \left(\frac{\theta-\theta_r}{\theta_s-\theta_r}\right) \left(1 - \left(1 - \left(\frac{\theta-\theta_r}{\theta_s-\theta_r}\right)^{\frac{1}{m}}\right)^{m}\right)^{2} \quad \textbf{Equation 3-2}$$

where α approximates the inverse of air entry pressure (L^{-1}), *n* is a fitting parameter related to the pore-size distribution, $m = 1-1/n$, θ_r is residual saturation, θ_s is the saturated water content, L is a fitting parameter related to tortuosity, and K_s is saturated hydraulic conductivity ($L\ T^{-1}$). The curves generated using Equations 3-1 and 3-2 will be referred to as VGM SWRC's and VGM hydraulic conductivity curves in the following sections.

3.3.3 Issues

Analysis of results collected from the laboratory column experiments revealed issues in the data that were difficult to account for. When comparing the assumed irrigation rate to logged outflow, it appeared that the tipping buckets were not accurately logging the data and underestimating the actual amount of water that was released from each column. Various scenarios were considered, however none of them were able to account for the large discrepancies and therefore it was assumed that issues with the tipping buckets went unnoticed and thus the data set has not been included in the results.

3.4 Results

3.4.1 Soil properties

Soil textural analysis determined that the LFH at all three study sites could all be classified as loam, but their subsoils differed (Table 3-1). Subsoils were classified as silt loam, loam and sand at the 11, 8 and 6-year sites, respectively. The layering of textures also differed between sites. The 11 and 8-year sites were constructed so that a coarser soil (LFH) was placed over a finer soil (subsoil). The 6-year site had the opposite arrangement, with LFH being finer than its sandy subsoil. Bulk density of the 11 and 8-year sites were similar (0.93 and 0.88 g cm^{-3}, respectively), while that of the 6-year site was much higher (1.31 g cm^{-3}). Similarly, K_{sat} at the 11 and 8-year sites matched (2 x 10^{-4} m s^{-1}), whereas at the 6-year site was much lower (6 x 10^{-6} m s^{-1}). The depth of LFH at the 6 and 8-year sites (23 and 12 cm, respectively) was less than the designed soil prescriptions of 30 and 20 cm, respectively.

Table 3-1- Average soil physical properties for LFH and subsoil at all study sites. # of samples = 9 for LFH and 1 for subsoil. *Values for 6-year subsoil SSC, bulk density and porosity are from Ketcheson (2015). 6-year LFH and subsoil K_{sat} was estimated using the ROSETTA pedotransfer function.

Property	Site					
	11-year		8-year		6-year*	
	LFH	Subsoil (Till)	LFH	Subsoil (Till)	LFH	Subsoil (Tailings sand)
Layer depth (cm)	21	24	12	33	23	22
Infiltration rate (mm hr^{-1})	803	N/A	810	N/A	93	N/A
K_{sat} (m s^{-1})	2 x 10^{-4}	5 x 10^{-7}	2 x 10^{-4}	1 x 10^{-7}	6 x 10^{-6}	4 x 10^{-5}
ρ_b (g cm^{-3})	0.93	1.30	0.88	1.5	1.31	1.45
Porosity (cm^3/cm^3)	0.59	0.43	0.60	0.43	0.5	0.45
Sand (%)	42	23	55	45	51	88
Silt (%)	35	64	37	30	41	11
Clay (%)	22	12	8	26	8	1
Soil textural class	Loam	Silt Loam	Loam	Loam	Loam	Sand
θ_r	0.06	0.04	0.04	0.05	0.05	0.04
θ_s	0.53	0.39	0.50	0.33	0.41	0.40
α	3.54	1.18	1.84	1.41	0.94	4.07
n	1.36	1.18	1.34	1.26	1.52	2.48

The measured soil water retention curves and the VGM SWRC's match relatively well when comparing *VWC* and the patterns observed between sites and materials (

Figure 3-2). The greatest discrepancies between the measured and VGM curves were observed in the 11-year subsoil, particularly at the 1, 5 and 10 m pressure steps, where there was a difference in *VWC* of approximately 0.09. *VWC* at all other pressure steps for the other sites and materials presented in Figure 3-2 were typically within 0.05 of the measured retention curves for all pressure steps.

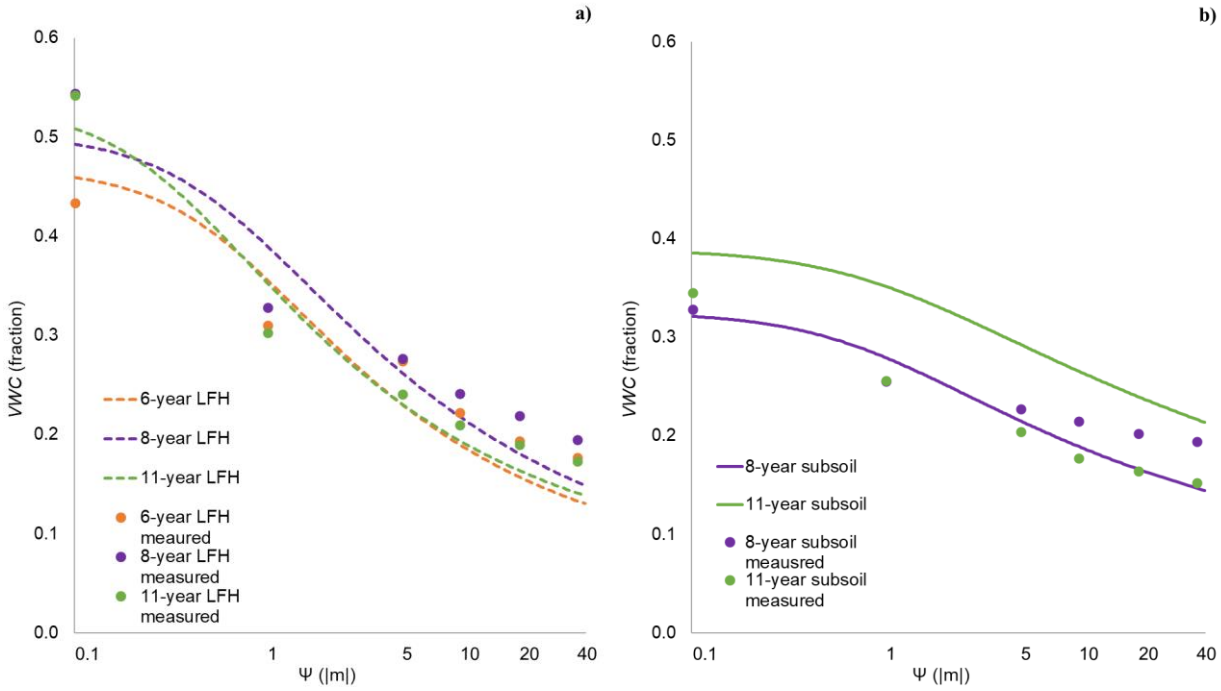

Figure 3-2 – Comparison of VGM SWRC's and measured SWRC's. a) presents results for LFH from all three sites and b) presents results for subsoil. VGM curves were generated using equations 3-1 and 3-2 and the van Genuchten parameters α, n, θ_s and θ_r that were estimated using ROSETTA. # of sample for curves that represent LFH = 9, and 1 for subsoil. The x-axis has been presented on a log scale to allow for easier comparison between the two data sets. Measured retention data were not available for the 6-year subsoil.

3.4.2 Van Genuchten soil water retention and hydraulic conductivity curves

The VGM SWRC's and hydraulic conductivity curves for LFH from all study sites (Figure 3-3) are all similar in shape as a result of their common textural classifications (Table 3-1). The finer textures of the 8 and 11-year sites' subsoils, relative to LFH are reflected by their shallower SWRC's (Figure 3-3, a). In contrast, the SWRC of the 6-year sites' sandy subsoil is steeper, indicative of its coarser texture. Considering the possibility of a capillary barrier at an LFH-tailings sand interface, the breakthrough head (ψ_B) of the 6-year sites tailings sand was determined to be 0.2 m by locating the inflection point of its VGM SWRC. The breakthrough head corresponds to the *VWC* required in the LFH (θ_{LFH}) and subsoil ($\theta_{\mathrm{subsoil}}$) to breach the capillary barrier (Khire et al., 2000). θ_{LFH} was 0.44 in the 6-year LFH, which is similar to its value for θ_{s} (0.41), estimated using the ROSETTA PTF.

For both the 8 and 11-year sites, *K(ψ)* is two to three orders of magnitude higher in the LFH compared to the 8 and 11-year subsoils, except for at pressures not expected in the field (> 200 m) (Figure 3-3, b). *K(ψ)* of the 6-year sites' subsoil is several orders of magnitude lower than its overlying LFH until pressure approaches the breakthrough head of 0.2 m. Once the breakthrough head has been achieved, *K(ψ)* of the 6-year subsoil (2×10^{-2} m s^{-1}) surpasses that of the 6-year LFH (7×10^{-3} m s^{-1}), creating conditions for breakthrough to occur.

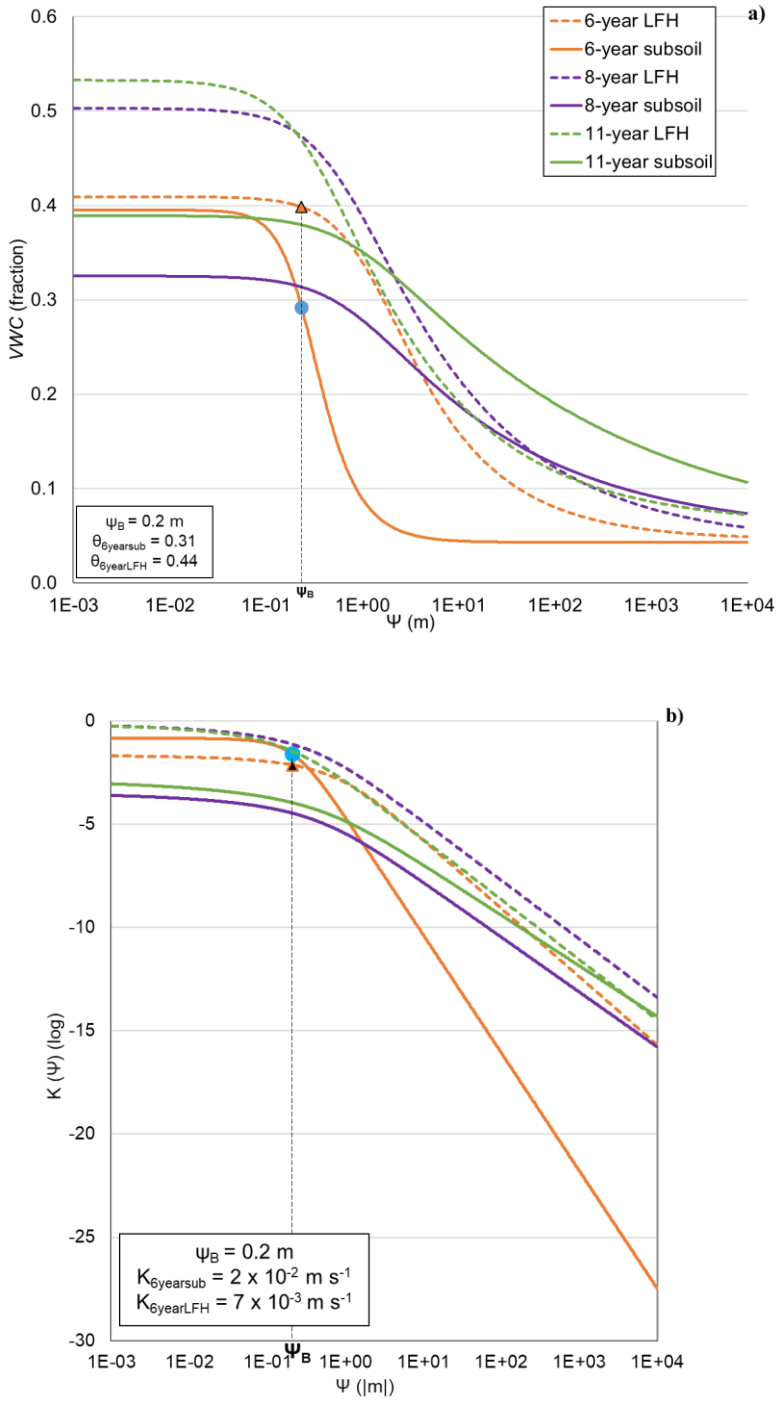

Figure 3-3 - Soil water retention and hydraulic conductivity curves generated using the estimated VGM parameters and equations 3-1 and 3-2. The blue dot on the 6-year subsoil curves indicates the position of the breakthrough head (0.2 m), determined by locating the tailings sand SWRC's inflection point. The triangles on the 6-year LFH curves indicate 0.2 m and the corresponding values for *VWC* and *K(ψ)* (indicated in box).

3.4.3 Laboratory column experiments

Table 3-2- Changes to soil water storage during laboratory column experiments.

Site	Layer Intervals (cm)			Change in Storage (mL)											
				Irrigation 1 (3450 mL)			Irrigation 2 (6900 mL)			Irrigation 3 (10350 mL)			Cumulative (20700 mL)		
	11-year	8-year	6-year	11-year	8-year	6-year	11-year	8-year	6-year	11-year	8-year	6-year	11-year	8-year	6-year
LFH	0-10	0-5	0-10	707	389	778	0	35	0	0	106	0	707	530	778
	10-21	5-12	10-23	707	445	509	71	49	85	141	0	0	919	495	594
Total				**1414**	**834**	**1286**	**71**	**85**	**85**	**141**	**106**	**0**	**1626**	**1025**	**1371**
Subsoil	12-27	12-22	23-32	198	283	495	247	71	1484	0	0	0	445	353	1979
	27-45	22-45	32-45	763	650	643	509	0	1838	127	0	0	1400	650	2481
Total				**961**	**933**	**1138**	**756**	**71**	**3322**	**127**	**0**	**0**	**1845**	**1004**	**4460**
Total Change in Storage				2375	1767	2425	827	156	3407	269	106	0	3471	2029	5832
Estimated Outflow				1075	1683	1025	6073	6744	3493	10081	10244	10350	17229	18671	14868
Outflow / Irrigation (%)				31	49	30	88	98	51	97	99	100	83	90	72

The following figures (Figure 3-4, Figure 3-5 and Figure 3-6) present the results from the laboratory column experiments and Table 3-2 above presents the changes to soil water storage within each column. For each layer, change in soil water storage was calculated for the period from immediately before the beginning of an irrigation event to immediately before the following irrigation event. Change in storage in each layer was determined by multiplying the change in *VWC* over the specified time period by the layer's depth in centimeters (cm) and the area of the column (707 cm^2) to obtain a value for change in storage in milliliters (mL). Estimated outflow was determined by assuming irrigation minus total change in storage was equal to outflow

11-year site

During the first irrigation event, a spike in *VWC* occurred in the LFH and a smaller spike occurred in the subsoil (Figure 3-4). After irrigation stopped, *VWC* declined in both materials, however the decline observed in the subsoil was minimal, particularly at the 24 cm probe. The resulting change in soil-water storage attributed to the first irrigation event was 1414 mL and 961 mL in the LFH and subsoil, respectively (Table 3-2). Change in soil water storage was calculated for the period from immediately before the beginning of an irrigation event to immediately before the following irrigation event. During the second and third irrigation events, large spikes in *VWC* occurred in the subsoil, in particular at the 24 cm probe, surpassing *VWC* measured in the LFH while water was being irrigated. In contrast to the first irrigation event, the resulting change in soil water storage attributed to the second irrigation event was much larger in the subsoil (756 mL mm) than in the LFH (71 mL). The third irrigation event resulted in minimal change in storage in both the LFH (141 mL) and subsoil (127 mL). Cumulatively, the majority of the change in soil-water storage in the LFH occurred during the first irrigation event and during the first and second event in the subsoil, for a total change in soil water storage of 1626 mL in the LFH and 1845 mL in the subsoil.

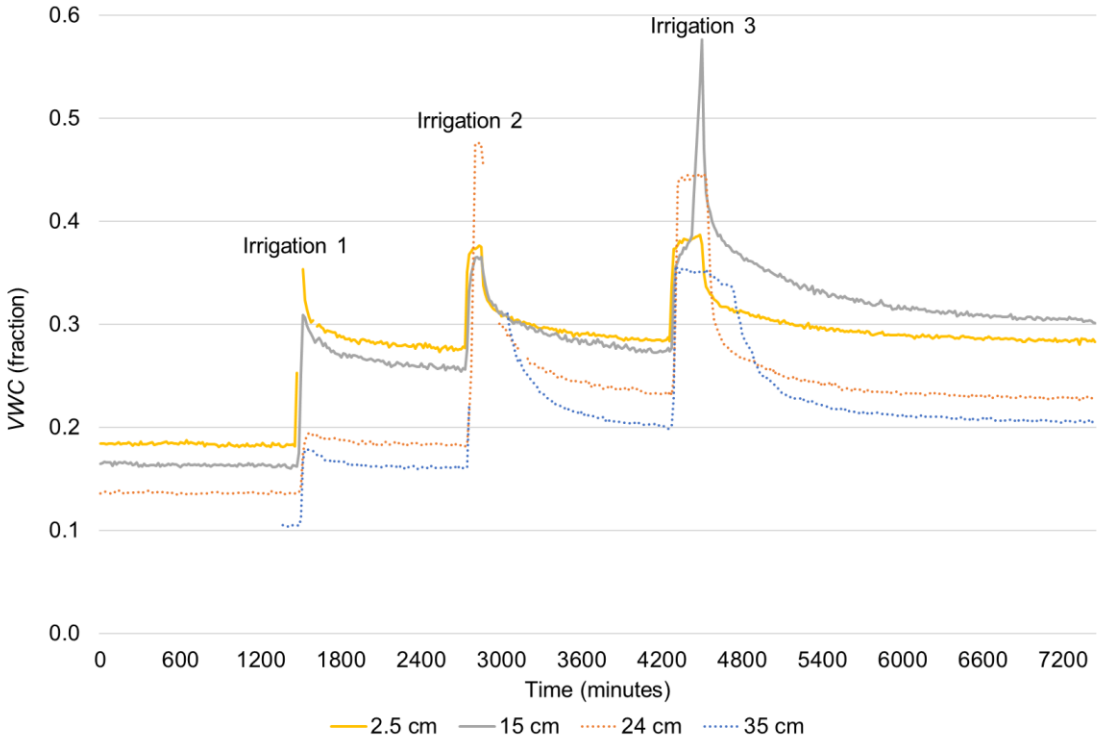

Figure 3-4 - Results from 11-year site laboratory column experiment. Solid lines represent soil moisture probes in LFH and dotted lines represent probes in subsoil.

8-year site

During the first irrigation event, a spike in *VWC* was observed in both the LFH and subsoil, however the magnitude of change in *VWC* was greater in the LFH (Figure 3-5). Following irrigation, *VWC* quickly declined at the 2.5 cm, 9 cm and 15 cm probes. At the 35 cm probe the increase in *VWC* was sustained for approximately 330 minutes. The resulting change in soil-water storage attributed to the first irrigation event was 834 mL and 933 mL in the LFH and subsoil, respectively (Table 3-2). During the second and third irrigation events, similar patterns in *VWC* were observed at all probes, however there was minimal change in soil-water storage in both the LFH and subsoil. Ponding was observed on top of the monolith during both the second and third irrigation events. Cumulatively, most of the change in storage occurred during the first irrigation event in both the LFH and subsoil.

Figure 3-5 - Results from 8-year site laboratory column experiment. Solid lines represent soil moisture probes in LFH and dotted lines represent probes in subsoil.

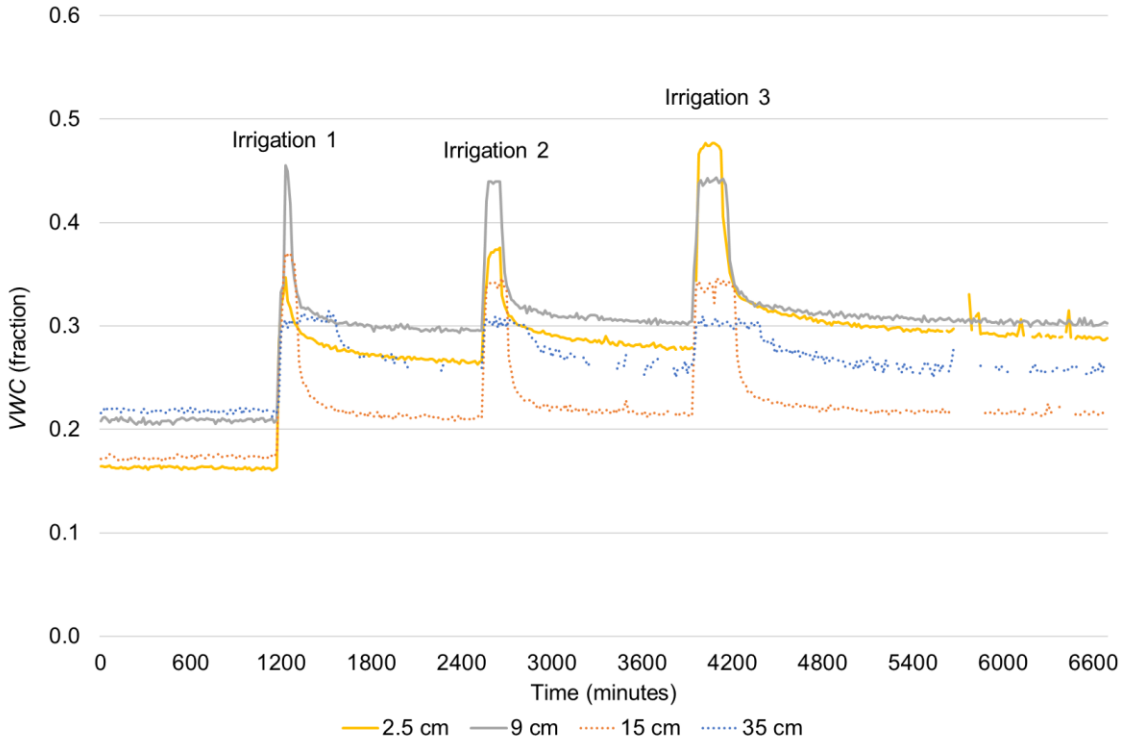

6-year site

During the first irrigation event, a spike in *VWC* was observed in the LFH and subsoil, however the magnitude of change was much greater in the LFH (Figure 3-6). Shortly after irrigation, *VWC* at the 2.5, 19 and 27 cm probes quickly fell while *VWC* at the 35 cm probe remained at the increased value. The resulting change in soil-water storage was 1286 mL in the LFH and 1138 mL in the tailings sand. During the second irrigation event, *VWC* in the LFH peaked to similar values as in the first irrigation event, and quickly fell once irrigation stopped, however the change in soil water storage was minimal at 85 mL. In contrast to the first event, *VWC* in the tailings sand increased a substantial amount. *VWC* at the 27 cm probe started to slowly decrease after irrigation was stopped, however, *VWC* at the 35 cm probe remained at the increased value. The total change in soil-water storage of the tailings sand attributed to the second irrigation event was 3322 mL During the third irrigation event *VWC* again peaked and fell in the LFH, yet remained relatively consistent in the tailings sand, and there was no change in soil-water storage in both the LFH and tailings sand. The *VWC* that corresponds to the

breakthrough head (0.2 m, 0.31) was reached and surpassed in the tailings sand during the second and third irrigation event, however it was never achieved in the LFH near the interface where it peaked at approximately 0.35.

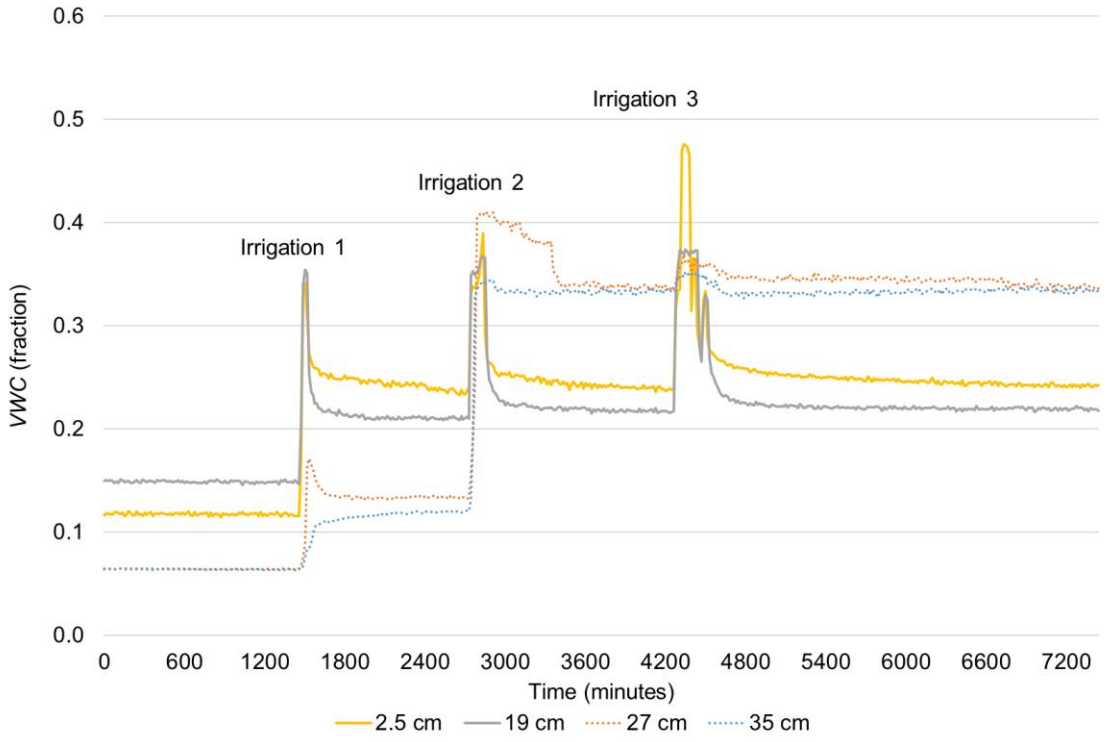

Figure 3-6 - Results from 6-year site laboratory column experiment. Solid lines represent soil moisture probes in LFH and dotted lines represent probes in subsoil.

3.5 Discussion

3.5.1 Expected vs. actual performance of layered soil profiles

The VGM soil water retention (SWRC) and hydraulic conductivity curves generated using Equations 3-1 and 3-2 provide some insight to the expected hydrological functioning of each study site and are reflective of the way they were constructed (Figure 3-3). The 8 and 11 – year sites, both constructed using saline-sodic overburden, were designed to mitigate the movement of contaminants associated with the overburden by placing a 100 cm layer of subsoil between it and the LFH. As a result of the contrasting textures of the LFH (coarser) and subsoil (finer), and thus their hydraulic properties, the

estimated hydraulic conductivity of the subsoils are two to three orders of magnitude lower than the overlying LFH, at any given soil-water pressure that would be expected in the field (Figure 3-3, b). This arrangement of hydraulic conductivities (LFH > subsoil) is indicative of a hydraulic barrier that limits percolation across the interface of two materials as water moving through the more conductive overlying material is restricted by the less conductive underlying material (Li et al., 2014).

In contrast to the 8 and 11-year sites, the 6-year site was constructed using coarser tailings sand overlain by finer LFH. This arrangement of a finer material over a coarser material can result in a capillary barrier that mitigates percolation across an interface due to the lower permeability of the coarser material under unsaturated conditions (Yang et al., 2004). Further, the VGM SWRC and hydraulic conductivity curves obtained for the 6-year LFH and subsoil, point to the presence of a capillary barrier at the 6-year site (Figure 3-3, b). At the breakthrough head (0.2 m), $K(\psi)$ in the 6-year LFH (7×10^{-3} m s^{-1}) becomes less than in the tailings sand (2×10^{-2} m s^{-1}), theoretically allowing water to quickly move across the interface.

Results collected from the laboratory column experiments partially support the expected findings from the VGM soil water retention and hydraulic conductivity curves. And, although the high irrigation rate made it difficult to evaluate the true performance of the soil profiles under realistic soil moisture conditions, the results collected are useful in evaluating the accuracy of the VGM soil water retention and hydraulic conductivity curves. The 11-year site had a somewhat effective barrier at the LFH-subsoil interface during the first irrigation event (Figure 3-4). The greater change in soil-water storage in the LFH compared to subsoil and large difference in *VWC* between the two materials is evidence that irrigated water was held above the interface after the first irrigation event. The rate of decline in *VWC* in the LFH after irrigation suggests the presence of a hydraulic barrier as opposed to a capillary barrier. In the presence of a capillary barrier, *VWC* in the overlying material would decline at a quicker rate due to the rapid increase in permeability in the underlying material associated with the breakthrough head (Stormont and Anderson, 1999; Sutton and Price, 2019). During the second irrigation event the hydraulic barrier was weakened as evidenced by the spike in *VWC* in the subsoil that surpassed the *VWC* measured in the LFH. Despite sharing similar soil physical properties to the 11-year site, the expected hydraulic barrier at the 8-year site was ineffective during all three irrigation events. Even under the lowest irrigation amount (Irrigation 1), the expected hydraulic barrier at the LFH-subsoil interface in the 8-year monolith did not mitigate a substantial amount of percolation across the interface (Figure 3-5). The spike in *VWC* in the subsoil and comparable change in soil-water storage in the LFH (834 mL) to the subsoil (933 mL) (Table 3-2) indicate that most of the

irrigated water was removed from the LFH and entered the underlying subsoil. In the second and third irrigation events smaller changes in soil-water storage further point to an ineffective barrier.

Column experiment results from the 6-year site did not show evidence of the expected capillary barrier at the interface (Figure 3-6). After the first irrigation event there was a large gap in *VWC* in the LFH compared to the subsoil, however, there was a similar change in soil water storage in both materials (1286 mL and 1138 mL, respectively), suggesting there was some hydraulic connectivity between the two layers and, if there was a capillary barrier, it was weak. This may be an artefact of the drying that occurred between sampling and the experiment, or perhaps the small increase was due the presence of preferential flow pathways such finger flow (Hillel and Baker, 1988), or small fractures that were introduced during monolith extraction the field. Despite this, the VGM SWRC and hydraulic conductivity curves are reflective of the 6-year site based on other studies at the same location. The presence of a capillary barrier at the 6-year site has been verified by Sutton and Price (2019) who determined that the approximate breakthrough head was 0.11 m using soil moisture data collected from the field, which corresponds well with the breakthrough head determined in this study (0.2 m).

3.5.2 Implications for reclamation

Layered soil profiles in a reclaimed landscape have the potential to impact the hydrological function of the landscape (Leatherdale et al., 2012; Huang et al., 2013; Naeth et al., 2011). Using easily obtained soil physical properties, it is possible to predict whether a barrier is expected as well as its type and effectiveness. Even under high irrigation amounts, the expected percolation barriers at both the 6 and 11-year sites were reflected in the results collected from the laboratory column experiments. The ineffectiveness of the expected hydraulic barrier at the 8-year site is an important consideration as well. Given the similar soil physical properties to the 11-year site, it is possible that preferential flow pathways within the monolith were responsible for the relatively high connectivity between the LFH and subsoil (Bogner et al., 2010), something that would not have been captured by the analysis done in this study, emphasizing the spatial variability in soil conditions at the same reclamation site.

Different percolation barriers (hydraulic or capillary) have different implications for landscape function. In the case of LFH overlying subsoil comprised of glacial till (8 and 11-year sites), a common arrangement for overburden dumps, a hydraulic barrier will benefit the landscape as water is held above the interface for longer durations. This has been shown to artificially increase field capacity in the overlying soil, and thus available water holding capacity, water that is available

for plant use (Huang et al., 2013; Zettl et al., 2011). This also supports the goal of an overburden dump to reduce net percolation into the subsurface in an effort to mitigate the movement of contaminants associated with the saline-sodic overburden used in their construction (Barber et al., 2015). The presence of a capillary barrier, such as the one detected at the 6-year site, would have similar implications as a hydraulic barrier, specifically during drier periods when the overlying LFH remains dry enough so that the breakthrough head is not achieved. However, once a capillary barrier is broken through, water is released into the subsurface and the materials remain hydraulically connected until soil moisture conditions return to pre-breakthrough levels (Stormont and Anderson, 1999). Thus, in landscapes where connectivity between the surface cover and subsoil are necessary for success, such as the upland of an upland-fen watershed (6-year site), the unique behaviour of a capillary barrier could be of benefit to vegetation while also promoting recharge, so long as soil moisture conditions to allow breakthrough are periodically achieved.

While laboratory data can give insight to the behaviour of a soil profile at a moment in time, it is necessary to consider the dynamic nature of soils. Biotic and abiotic forces can alter a soil's structure post-placement and thus alter certain physical properties, such as K_{sat} and soil-water retention (Benson et al., 2007; Meiers et al., 2011). Expected changes to the van Genuchten parameters with time (*e.g.* increase in α) (Benson et al., 2007) would result in a lower *VWC* associated with the breakthrough head of the underlying tailings sand (Sutton and Price 2019). Since the breakthrough *VWC* in the LFH would become lower as the soil evolves, the capillary barrier would be weaker and conditions for percolation into the subsurface would occur more frequently.

3.5.3 Errors and limitations

Certain errors and limitations should be taken into consideration along with the results from this study. First, only one monolith was used for each site, eliminating the possibility to capture the spatial variability in soil properties across a reclamation site. In relation to this, only one subsoil sample was taken along with each monolith; and while a total of 9 LFH samples were used to characterize the LFH properties, they represented an average of the site, rather than the exact location the monolith and subsoil samples were collected. This could lead to errors in comparisons made between the VGM SWRC and hydraulic conductivity curves, and results from the laboratory column experiments. Finally, since no subsoil sample was collected from the 6-year site its properties had to be estimated or retrieved from other sources and thus is not consistent with methods used for the 8 and 11-year sites.

The discrepancies between expected function based on the VGM hydraulic conductivity curves compared to the laboratory column experiment data further illustrate the spatial variability of a reclamation site and highlight the need to evaluate and consider other processes within the soil profile that could impact the hydraulic connectivity between two materials. For instance, these column experiments did not consider the possibility of preferential flow pathways (e.g. macropore flow or finger flow), that may have connected the two materials, contributing to results that were not reflective of the VGM hydraulic conductivity curves.

3.6 Conclusion

While not necessarily intentional, percolation barriers in a layered soil profile constructed using LFH mineral mix are a likely occurrence. Their impact on hydrological functioning depends on the type of barrier (hydraulic vs capillary) as well as the intended function of the landscape. In spite of the high irrigation rate of the laboratory column experiments, which made it difficult to assess in detail the performance of the soil profiles within the monoliths, the data was valuable in confirming the use of more easily obtained laboratory data and a pedotransfer function, such as ROSETTA. With the VGM soil water retention and hydraulic conductivity curves it was possible to predict the presence of a percolation barrier as well as how it may behave in the field (determination of breakthrough head for a capillary barrier). However, the possibility of spatially distinct preferential flow pathways across an interface as well as the temporal evolution of soils should be considered along with their use.

Chapter 4
Conclusion

LFH mineral mix is a dynamic material that varies considerably both spatially and temporally. Its use for reclamation in the AOSR has been well documented, in particular its suitability as a substrate for revegetation. The current study aimed to develop a better understanding of its impact on the hydrological functioning of a landscape, both near the surface and in its interactions with underlying materials.

The dynamic nature of LFH of supports the use of LFH of lower initial quality (*e.g.* low infiltration, low soil organic matter, high bulk density), so long as best management practices to ensure the establishment and growth of vegetation in the early years of reclamation are employed. With the growth of vegetation, certain properties in LFH (*e.g.* van Genuchten α) should continue to improve with time, leading to the continual development of larger pores within LFH, even after the effects of abiotic forces such as freeze-thaw cycling have lessened. This will improve hydrologic response, benefiting landscapes where groundwater recharge is necessary for success (*e.g.* upland-fen watershed). Although LFH with high values for soil organic matter and lower values for bulk density (i.e. higher quality) did seem to instigate "quicker" success in reclamation, based on natural canopy regeneration; sites capped with lower quality LFH were still functioning uplands as evidenced by the development of vegetation despite issues with seedling mortality in early years of reclamation.

In landscapes where percolation into the subsurface is not beneficial (*e.g.* overburden dumps), the hydrophysical evolution of LFH is a potential hinderance, however the manner in which these landscapes are constructed can counteract this. In these landscapes, coarser LFH placed over finer subsoil (*e.g.* glacial till) is likely to form a hydraulic barrier to percolation as a result of the restrictive nature of the subsoil's low hydraulic conductivity, as long as the differences in hydraulic conductivity are great enough. In this study there was a two order of magnitude difference between $K(\psi)$ in the LFH (faster) and subsoil (slower) that formed an effective hydraulic barrier at the 11-year site. In the opposite arrangement where LFH is placed over a relatively coarser material (*e.g.* tailings sand), a capillary barrier may form, even if the difference between K_{sat} is only one order of magnitude. Both a hydraulic and capillary barrier can be of benefit to vegetation as water is held above the interface of the two materials, increasing field capacity and thus available water holding capacity. However, in the case of a capillary barrier, when breakthrough soil moisture conditions are met (near saturation), the two materials would become hydraulically connected, allowing water to enter the underlying tailings

sand until pre-breakthrough conditions are established as the soil dries out. The unique behaviour of a capillary barrier could benefit a landscape such as the upland of an upland-fen watershed. During drier periods water would be held above the interface and thus more readily available to plants, but when conditions allow, percolation events will occur.

The use of ROSETTA and RET-C in Chapter 2 to estimate the van Genuchten parameters and associated properties highlight the differences between the two methods. Although RET-C did provide a better fit to the measured retention data, ROSETTA was able to capture the expected patterns with time in hydraulic properties (increasing α), that RET-C was unable to. In Chapter 3, ROSETTA was able to partially predict the expected function of layered soil profiles, reflected in the laboratory column experiment for the 11-year site and the capillary barrier that has been observed in the field at the 6-year site. These findings warrant further research into the validity of ROSETTA for use in parameter estimation necessary for modelling the behaviour of materials used in land reclamation in the AOSR.

Future study to enhance the results presented here could identify thresholds for effective percolation barriers (minimum difference in hydraulic conductivities) as well as identify the impact that changing soil conditions could have on the effectiveness of a barrier. For instance, as vegetation becomes more established roots may enter the subsoil, creating preferential flow pathways and thus the possibility of enhanced hydraulic connectivity between the two materials. Further, long term studies on the evolution of LFH at a particular reclamation site, as has been done with peat-mineral mix (PMM), would be beneficial in verifying results presented in Chapter 2 as well as potentially capture changes to LFH that may occur over longer periods of time (*e.g.* intrinsic properties upon placement) and their associated impact on site function.

References

Addo-Danso, S. D., Prescott, C. E., & Smith, A. R. (2016). Methods for estimating root biomass and production in forest and woodland ecosystem carbon studies: A review. *Forest Ecology and Management*, *359*, 332–351. https://doi.org/10.1016/j.foreco.2015.08.015

Alberta Environment. (2006). *Land Capability Classification System for Forest Ecosystems in the Oil Sands, 3rd Edition* (Vol. 1).

Alberta Environment. (2010). *Guidelines for Reclamation to Forest Vegetation in the Athabasca Oil Sands Region, 2nd Edition*.

Barber, L. A., Bockstette, J., Christensen, D. O., Tallon, L. K., & Landhausser, S. M. (2015). Effect of soil cover system design on cover system performance and early tree establishment. *Mine Closure*, 1–9.

Benson, C. H., Sawangsuriya, A., Trzebiatowski, B., & Albright, W. H. (2007). Pedogenic Effects on the Hydraulic Properties of Water Balance Cover Soils, *133*(4), 349–359.

Benson, H. (1992). Effect of freeze-thaw on the hydraulic conductivity and morphology of compacted clay.

Bogner, C., Gaul, D., Kolb, A., Schmiedinger, I., & Huwe, B. (2010). Investigating flow mechanisms in a forest soil by mixed-effects modelling. *European Journal of Soil Science*, *61*(6), 1079–1090. https://doi.org/10.1111/j.1365-2389.2010.01300.x

Bradshaw, A. (1997). Restoration of mined lands—using natural processes. *Ecological Engineering*, *8*(4), 255–269. https://doi.org/10.1016/S0925-8574(97)00022-0

Brown, R. L., & Naeth, M. A. (2014). Woody debris amendment enhances reclamation after oil sands mining in Alberta, Canada. *Restoration Ecology*, *22*(1), 40–48. https://doi.org/10.1111/rec.12029

Devito, K., Mendoza, C., Qualizza, C. (2012). *Conceptualizing Water Movement in the Boreal Plains. Implications for watershed reconstruction. Synthesis report prepared for the Canadian Oil Sands Network for Research and Development, Environmental and Reclamation Research Group*. https://doi.org/10.1017/CBO9781107415324.004

Dexter, a R. (2004). Soil physical quality Part I. Theory, effects of soil texture, density, and organic

mailer, and effects on root growth. *Geoderma*, *120*, 201–214. https://doi.org/10.1016/j.geodermaa.2003.09.005

Dhar, A., Comeau, P. G., Karst, J., Pinno, B. D., Chang, S. X., Naeth, A. M., … Bampfylde, C. (2018). Plant community development following reclamation of oil sands mine sites in the boreal forest : a review, *298*(May), 286–298.

Dingman, S. . (2015). *Physical hydrology*. *Physical Hydrology* (3rd ed.). Long Grove, IL: Waveland Press, Inc. https://doi.org/10.1177/030913337800200111

Elshorbagy, A., Jutla, A., Barbour, L., & Kells, J. (2005). System dynamics approach to assess the sustainability of reclamation of disturbed watersheds 1, *158*, 144–158. https://doi.org/10.1139/L04-112

Genuchten, M. T. Van. (1980). A Closed-form Equation for Predicting the Hydraulic Conductivity of Unsaturated Soils. *Soil Science Society of America Journal*, *44*(5).

Germann, P. (1982). Macropores and Water Flow in Soils, *18*(5), 1311–1325.

Hillel, D., & Baker, R. (1988). A Descriptive Theory of Fingering During Infiltration Into Layered Soils. *Soil Science*, *146*(1), 51–56. https://doi.org/10.1515/9781400828036.xiii

Houlbrooke, D. J., Thom, E. R., Chapman, R., Mclay, C. D. A., Thom, E. R., Chapman, R., & Mclay, C. D. A. A. (2010). A study of the effects of soil bulk density on root and shoot growth of different ryegrass lines, *8233*. https://doi.org/10.1080/00288233.1997.9513265

Huang, M; Barbour, S.L; Elshorbagy, A; Zettle, J; Si, B. . (2013). Effects of variably layered coarse textured soils on plant av ailable water and forest productivity. *Procedia Environmental Sciences*, *19*, 148–157. https://doi.org/10.1016/j.proenv.2013.06.017

Huang, M., Barbour, S. L., & Carey, S. K. (2015). The impact of reclamation cover depth on the performance of reclaimed shale overburden at an oil sands mine in Northern, *2854*(January), 2840–2854. https://doi.org/10.1002/hyp.10229

Jamro, G. M., Chang, S. X., & Naeth, M. A. (2014). Organic capping type affected nitrogen availability and associated enzyme activities in reconstructed oil sands soils in Alberta , Canada. *Ecological Engineering*, *73*, 92–101. https://doi.org/10.1016/j.ecoleng.2014.09.005

Karlen, D. L., Ditzler, C. A., & Andrews, S. S. (2003). Soil quality : why and how ?, *114*, 145–156. https://doi.org/10.1016/S0016-7061(03)00039-9

Kelln, C., Barbour, L., & Qualizza, C. (2007a). Preferential Flow in a Reclamation Cover : Hydrological and Geochemical Response, *133*(October), 1277–1289.

Kelln, C., Barbour, L., & Qualizza, C. (2007b). Preferential Flow in a Reclamation Cover: Hydrological and Geochemical Response. *Journal of Geotechnical and Geoenvironmental Engineering*, *133*(10), 1277–1289. https://doi.org/10.1061/(ASCE)1090-0241(2007)133:10(1277)

Kessler, S., Barbour, S. L., van Rees, K. C. J., & Dobchuk, B. S. (2010). Salinization of soil over saline-sodic overburden from the oil sands in Alberta. *Canadian Journal of Soil Science*, *90*(4), 637–647. https://doi.org/10.4141/cjss10019

Ketcheson, S. J. (2015). Hydrology of a Constructed Fen Watershed in a Post-Mined Landscape in the Athabasca Oil Sands Region, 180.

Ketcheson, S. J., Price, J. S., Carey, S. K., Petrone, R. M., Mendoza, C. A., & Devito, K. J. (2016). Constructing fen peatlands in post-mining oil sands landscapes: Challenges and opportunities from a hydrological perspective. *Earth-Science Reviews*, *161*, 130–139. https://doi.org/10.1016/j.earscirev.2016.08.007

Ketcheson, S. J., Price, J. S., Sutton, O., Sutherland, G., Kessel, E., & Petrone, R. M. (2017). The hydrological functioning of a constructed fen wetland watershed. *Science of the Total Environment*, *603–604*, 593–605. https://doi.org/10.1016/j.scitotenv.2017.06.101

Ketcheson, S., & Price, J. (2016). A comparison of the hydrological role of two reclaimed slopes of different age in the Athabasca Oil Sands Region, Alberta, Canada. *Canadian Geotechnical Journal*, *14*(August). https://doi.org/10.1139/cgj-2015-0391

Khire, B. M. V, Member, A., Benson, C. H., Member, A., & Bosscher, P. J. (2000). Capillary Barriers: Design Variables and Water Balance. *Journal of Geotechnical and Geoenvironmental Engineering*, 695–708.

Kosugi, K. (2002). Estimation of hydraulic properties of vertically heterogeneous forest soil from transient matric pressure data, *38*(12), 1–18. https://doi.org/10.1029/2002WR001546

Leatherdale, J., Chanasyk, D. S., & Quideau, S. (2012). Soil water regimes of reclaimed upland slopes in the oil sands region of Alberta, *1*. https://doi.org/10.4141/CJSS2010-027

Lewis, J., & Sjöstrom, J. (2010). Optimizing the experimental design of soil columns in saturated and

unsaturated transport experiments. *Journal of Contaminant Hydrology*, *115*(1–4), 1–13. https://doi.org/10.1016/j.jconhyd.2010.04.001

Li, X., Chang, S. X., & Salifu, K. F. (2014). Soil texture and layering effects on water and salt dynamics in the presence of a water table: A review. *Environmental Reviews*, *22*(1), 41–50. https://doi.org/10.1139/er-2013-0035

Mackenzie, D. (2011). *Best Management Practices For Conservation of Reclamation Materials in the Mineable Oil Sands Region of Alberta*. *Alberta Environment*. https://doi.org/978-1-4601-0048-6

Mackenzie, D. D., & Naeth, M. A. (2010a). The role of the forest soil propagule bank in assisted natural recovery after oil sands mining. *Restoration Ecology*, *18*(4), 418–427. https://doi.org/10.1111/j.1526-100X.2008.00500.x

Mackenzie, D. D., & Naeth, M. A. (2010b). The Role of the Forest Soil Propagule Bank in Assisted Natural Recovery after Oil Sands Mining, *18*(4), 418–427. https://doi.org/10.1111/j.1526-100X.2008.00500.x

Macyk, T. M. (2006). *Tailings Sand and Natural Soil Quality at the Syncrude Aurora, Albian Sands, CNRL, and Suncor Mines*.

McAdams, N.B; Quideau, S.A; Swallow, M; Lumley, L. . (2018). Oribatid mite recovery along a chronosequence of afforested boreal sites following oil sands mining. *Forest Ecology and Management*, *422*, 281–293.

Meiers, G. P., Barbour, L., Qualizza, C. V., & Dobchuk, B. S. (2011a). Evolution of the Hydraulic Conductivity of Reclamation Covers over Sodic/Saline Mining Overburden. *Journal of Geotechnical and Geoenvironmental Engineering*, *137*(10), 968–976. https://doi.org/10.1061/(ASCE)GT.1943-5606.0000523

Meiers, G. P., Barbour, L., Qualizza, C. V., & Dobchuk, B. S. (2011b). Evolution of the Hydraulic Conductivity of Reclamation Covers over Sodic/Saline Mining Overburden. *Journal of Geotechnical and Geoenvironmental Engineering*, *137*(10), 968–976. https://doi.org/10.1061/(ASCE)GT.1943-5606.0000523

Naeth, M. A., Chanasyk, D. S., & Burgers, T. D. (2011). Vegetation and soil water interactions on a tailings sand storage facility in the athabasca oil sands region of Alberta Canada. *Physics and Chemistry of the Earth*, *36*(1–4), 19–30. https://doi.org/10.1016/j.pce.2010.10.003

Naeth, M. A., Wilkinson, S. R., Mackenzie, D. D., Archibald, H. A., & Powter, C. B. (2013). *Potential of LFH Mineral Soil Mixes for Reclamation of Forested Lands in Alberta*.

Rillig, M. C., & Mummey, D. L. (2006). Mycorrhizas and soil structure. *New Phytologist*, 41–53.

Rooney, R. C., Bayley, S. E., & Schindler, D. W. (2012). Oil sands mining and reclamation cause massive loss of peatland and stored carbon. *Proceedings of the National Academy of Sciences of the USA*, *109*(13), 4933–4937. https://doi.org/10.1073/pnas.1117693108

Schaap, M. G., Leij, F. J., & Genuchten, M. T. Van. (2001). rosetta : a computer program for estimating soil hydraulic parameters with hierarchical pedotransfer functions, *251*, 163–176.

Scholl, P., Leitner, D., Kammerer, G., Loiskandl, W., Kaul, H. P., & Bodner, G. (2014). Root induced changes of effective 1D hydraulic properties in a soil column. *Plant and Soil*, *381*(1–2), 193–213. https://doi.org/10.1007/s11104-014-2121-x

Sorenson, P. T., Quideau, S. A., Mackenzie, M. D., Landhäusser, S. M., & Oh, S. W. (2011). Forest floor development and biochemical properties in reconstructed boreal forest soils. *Applied Soil Ecology*, *49*, 139–147. https://doi.org/10.1016/j.apsoil.2011.06.006

Stormont, J.C; Anderson, E. . (1999). Capillary Barrier Effect from Underlying Coarser Soil Layer. *Journal of Geotechnical and Geoenvironmental Engineering*, *125*(8), 641–648.

Sutton, O. F., & Price, J. S. (2019). Soil moisture dynamics modelling of a reclaimed upland in the early post-construction period. *Science of the Total Environment*.

Turcotte, I, Quideau, S; Oh, S. (2009). Organic matter quality in reclaimed boreal forest soils following oil sands mining. *Organic Geochemistry*, *40*, 510–519. https://doi.org/10.1016/j.orggeochem.2009.01.003

Twarakavi, N. K. C., International, Y., Sakai, M., & Simunek, J. (2009). An objective analysis of the dynamic nature of field capacity An objective analysis of the dynamic nature of field capacity, (October). https://doi.org/10.1029/2009WR007944

Weiler, M., & Naef, F. (2003a). An experimental tracer study of the role of macropores in infiltration in grassland soils, *493*(January 2002), 477–493. https://doi.org/10.1002/hyp.1136

Weiler, M., & Naef, F. (2003b). An experimental tracer study of the role of macropores in infiltration in grassland soils. *Hydrological Processes*, *493*(January 2002), 477–493. https://doi.org/10.1002/hyp.1136

Yang, F; Zhang, G; Yang, J; Li, D; Zhao, Y; Liu, F; Yang, R. (2014). Organic matter controls of soil water retention in an alpine grassland and its significance for hydrological processes. *Journal of Hydrology*, *519*, 3086–3093.

Yang, H., Rahardjo, H., Leong, E. C., & Fredlund, D. G. (2004). A study of infiltration on three sand capillary barriers. *Canadian Geotechnical Journal*, *41*(4), 629–643. https://doi.org/10.1139/T04-021

Zettl, J. D., Barbour, S. L., Huang, M., Si, B. C., & Leskiw, L. A. (2011). Influence of textural layering on field capacity of coarse soils. *Canadian Journal of Soil Science*, *91*(2), 133–147. https://doi.org/10.4141/cjss09117

Zoltai, S. C., Taylor, S., Jeglum, J. K., Mills, G. F., & Johnson, J. D. (n.d.). Wetlands of Boreal Canada.